Detection of Endoplasmic Reticulum Stress and Progression of Steatohepatitis in Mink (*Neovison vison*) with Fatty Liver

by

Catherine Pal

Submitted in partial fulfilment of the requirements
for the degree of Master of Science

at

Dalhousie University
Halifax, Nova Scotia

in co-operation with

Nova Scotia Agricultural College
Truro, Nova Scotia

August 2011

DALHOUSIE UNIVERSITY

NOVA SCOTIA AGRICULTURAL COLLEGE

The undersigned hereby certify that they have read and recommend to the Faculty of Graduate Studies for acceptance a thesis entitled "Detection of Endoplasmic Reticulum Stress and Progression of Steatohepatitis in Mink (*Neovison vison*) with Fatty Liver" by Catherine Pal in partial fulfilment of the requirements for the degree of Master of Science.

Dated: August 4, 2011

Supervisor: _____

Readers: _____

_____

_____

DALHOUSIE UNIVERSITY

AND

NOVA SCOTIA AGRICULTURAL COLLEGE

DATE: August 4, 2011

AUTHOR: Catherine Pal

TITLE: Detection of Endoplasmic Reticulum Stress and Progression of Steatohepatitis in Mink (*Neovison vison*) with Fatty Liver

DEPARTMENT OR SCHOOL: Department of Plant and Animal Science

DEGREE: MSc CONVOCATION: October YEAR: 2011

_____

Signature of Author

TABLE OF CONTENTS

LIST OF TABLES

LIST OF FIGURES

ABSTRACT

This study used the non-alcoholic steatohepatitis activity index (NAI), presence of fibrosis and Mallory-Denk bodies (MDBs), and quantification of glucose regulated protein 78 (GRP78) messenger ribonucleic acid (mRNA) as indicators of steatohepatitis development and recovery in the American mink (*Neovison vison*). Mink were fasted for 0, 1, 3, 5, or 7 days, and one group re-fed 28 days post 7-day fast. Liver NAI indicated that moderate fatty liver developed after 5 days of fasting. Liver recovery was achieved after the re-feeding period. There was no evidence of fibrosis or MDB formation. Up-regulation of GRP78 was observed by day 7 of fasting indicating endoplasmic reticulum stress. This effect was greater in females. Results suggest that liver steatosis did not advance to steatohepatitis within a 7-day fast. However, should the length of fast be increased the mink may be at risk. Results also show that liver recovery from simple fatty liver is possible.

LIST OF ABBREVIATIONS

ALLN	acetyl-leucyl-leucyl-norleucinal
ATF6	activating transcription factor 6
BW	body weight
CV	coefficient of variation
cDNA	complementary deoxyribonucleic acid
C_p	crossing point
C_t	cycle threshold
DNA	deoxyribonucleic acid
ER	endoplasmic reticulum
GO	glucose oxidase
GRP78	glucose regulated protein 78
GAPDH	glyceraldehyde-3-phosphate dehydrogenase
H&E	hematoxylin and eosin
HKG	housekeeping gene
Huh7	human hepatoma cells
BiP	immunoglobulin binding protein
MDB	Mallory-Denk body
mRNA	messenger ribonucleic acid
NAC	*N*-acetyl-cysteine
NCBI	National Center for Biotechnology Information
no RT	No reverse transcriptase
NAI	non-alcoholic steatohepatitis activity index
NAFLD	non-alcoholic fatty liver disease
NASH	non-alcoholic steatohepatitis
PCR	polymerase chain reaction
PCD	programmed cell death
PERK	protein kinase RNA-like endoplasmic reticulum kinase
qRT-PCR	quantitative real time polymerase chain reaction
ROS	reactive oxygen species
RF	re-feeding group
RNA	ribonucleic acid
rRNA	ribosomal RNA
TNF-α	tumor necrosis factor alpha
UPS	ubiquitin-proteasome system
UPR	unfolded protein response

ACKNOWLEDGEMENTS

I would first and foremost like to thank my advisor, Dr. Kirsti Rouvinen-Watt, for her guidance, support, and encouragement during my studies. I would also like to acknowledge the support and aid of my committee members, Dr. Leslie MacLaren and Dr. Lori Parsons. I would like to extend sincere thanks to the Histopathology lab team at the Atlantic Veterinary College, PEI for the training and support that I received there in histological techniques. I also would like to thank the Carnivore Nutrition and Physiology Lab group, especially Lora Harris. Thank you Lora for spending so many hours working with me to develop and run the qRT-PCR assay and for taking me out for coffee the many times when you realized that I needed a break. I would also like to thank Dr. Tess Astatkie for his statistical expertise. Thank you for your patience and the time that you spent helping me to develop my SAS programs, run my stats, and discussing the output with me.

I also like to sincerely thank my mother for her love and support during my entire scholastic career. I am a very lucky daughter to have such a wonderful mom.

This research was supported by grants from the Natural Sciences and Engineering Research Council (Discovery Grant to Dr. Rouvinen-Watt), the Canada Mink Breeders' Association and the Nova Scotia Department of Agriculture Technology Development Program (DEV26-001). Lastly, I would like to acknowledge the financial support received from the following scholarships during my studies: the Agriculture and Agri-Food Canada and Nova Scotia Department of Agriculture Graduate Research Training Initiative Scholarship, the Nova Scotia Fur Institute Scholarship, and the Canada Mink Breeders' Association Arlen Kerr Memorial Scholarship.

CHAPTER 1: INTRODUCTION

The liver is an essential organ involved in almost all biochemical processes in the body, including fat metabolism. Fatty liver is one of the largest causes of unplanned mortality in mink annually (Hunter and Barker 1996) and is a common pathological finding during the post mortem examination of females diagnosed with nursing sickness (Clausen et al. 1992). The development of fatty liver in mink is usually asymptomatic and rapid (Hunter and Barker 1996; Bjornvad et al. 2004). Animals often die before treatment can be administered. A greater understanding of the disease development and pathophysiology, which may be modelled by purposely fasting mink, will be beneficial as it will aid in the development of preventative procedures and treatments.

While development of simple fatty liver in response to fasting has been reported in mink (Bjornvad et al. 2004; Mustonen et al. 2005a), progression from simple fatty liver to the more severe and life threatening steatohepatitis, accumulation of fat along with induction of the inflammatory response, has not been identified in mink. Mallory-Denk bodies (MDBs), and development of fibrosis, are considered the morphologic hallmark of steatohepatitis in humans (Brunt et al. 1999). They could be applied to the study of the timescale of steatohepatitis development in mink. Studies by Hanada et al. (2007) and Lee (2005) suggest that oxidative stress and the endoplasmic reticulum (ER) resident chaperone glucose regulated protein 78 (GRP78) are associated with ER stress and play a role in MDB formation in human liver disease. Activation of the unfolded protein response (UPR) in the liver as a result of ER stress is a key feature in the development of steatohepatitis (Videla et al. 2004), insulin resistance, and type-2 diabetes (Özcan et al. 2004). Recent research into the disease mechanisms and pathophysiology

of mink nursing sickness suggests that they are associated with the development of insulin resistance and share characteristics that are similar to type-2 diabetes in humans (Rouvinen-Watt 2003; Hynes and Rouvinen-Watt 2007ab).

It is not known if or how quickly simple fat accumulation progresses to steatohepatitis in mink affected by fatty liver. Mallory-Denk body formation and the upregulation of GRP78 mRNA in the livers of fasted mink may be important indicators of ER stress leading to cellular dysregulation, induction of intracellular protein degradation mechanisms, and the development of steatohepatitis. The elimination of MDBs and the return of GRP78 mRNA levels to baseline may have the potential to be used to characterize liver recovery.

Better understanding of the time-scale of progression from simple fatty liver to steatohepatitis development will be very beneficial to mink producers, animal health care providers, and researchers. Knowing the critical time-point for intervention will help in the development of effective preventative and intervention therapies. Therefore, the purpose of this research is to characterize the timescale of progression of fatty liver disease to steatohepatitis through the identification of MDBs and presence of fibrosis in the liver and through mRNA quantification of the protein chaperone GRP78. Characterization of liver recovery from steatosis is also an objective.

CHAPTER 2.0: LITERATURE REVIEW

2.1 The Liver

The liver is the largest internal organ, normally accounting for nearly 2.5% of adult human body weight (Ross and Pawlina 2006), 3% of canine body weight, and between 1 and 1.5% body weight in horses and cows (Sjaastad et al. 2003). The liver normally accounts for about 4-6% of body weight in the mink (Juokslahti et al. 1978). It carries out approximately 1500 essential biochemical functions which affect growth, health, nutrient supply, energy production, and reproduction (Hand et al. 2000). It maintains homeostasis within the body through drug inactivation and detoxification, carbohydrate, lipid, and protein metabolism, production of bile for lipid breakdown, storage of nutrients (including glycogen, lipids, vitamins, and minerals), and through its role in the immune system (Cederbaum et al. 2004; Ross and Pawlina 2006). A basic understanding of liver physiology is essential to the understanding of liver pathology.

2.1.1 Liver Morphology

The liver is composed of lobules, each a roughly hexagonal structure composed of plates of parenchymal cells (hepatocytes), and non-parenchymal cells (Figure 1). Hepatocytes are the most numerous at 80% of the total liver volume and perform the majority of liver functions. Non-parenchymal cells, including Kupffer and stellate cells are located in the sinusoids. Non-parenchymal cells contribute to only 6.5% of liver volume but comprise 40% of the total number of liver cells (Kmiec 2001). Portal triads are located at lobule apices. The triad is the communal area where the portal vein and hepatic artery enter the liver and the bile duct exits. Within each lobule, the blood vessels traverse the periphery between the portal areas via the portal tracts. Branches from the

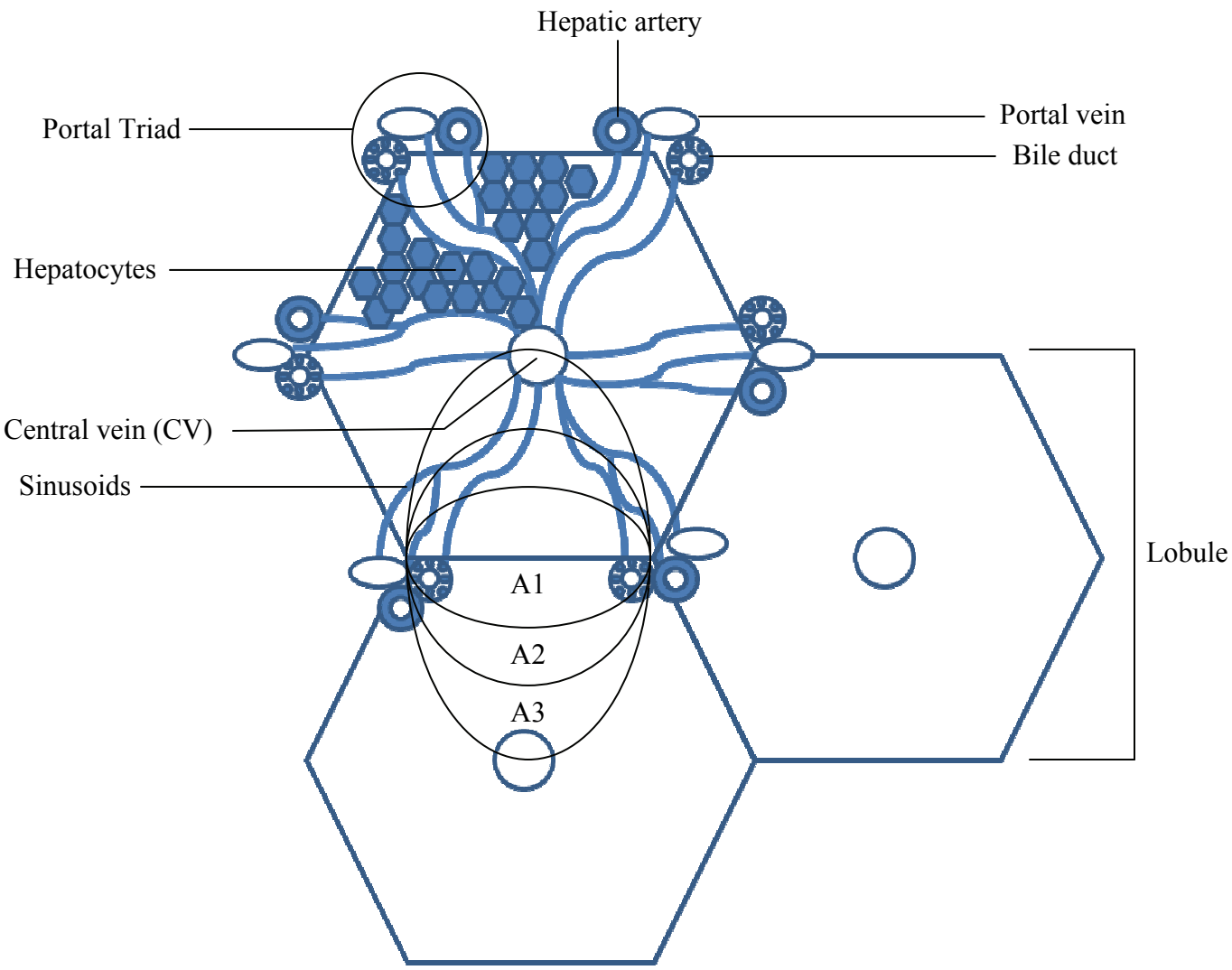

Figure 1. Schematic diagram of liver structure illustrating liver lobules. A1: Acinar zone 1, A2: Acinar zone 2, A3: Acinar zone 3.

periphery open into the hepatic sinusoids which travel from the outer edges of the lobule toward the central vein. The sinusoids are vascular channels that carry blood from the portal area to the central vein (Ross and Pawlina 2006). The plates of hepatocytes and the sinusoids are arranged in a radial pattern from the central vein to the edge of the lobule. This sets the oxygen gradient of the lobule; less oxygen is available to the hepatocytes the closer they are located to the central vein (Ross and Pawlina 2006). This oxygen gradient can effect which areas of the liver are affected earliest in the development of fatty liver disease and hence hepatic lipidosis sometimes has a controlobular pattern (Mantena et al. 2009). As the liver fills with fat and the sinusoids become narrower smaller volumes of oxygenated blood may reach the hepatocytes closest to the central vein (McCuskey et al. 2004). This may be a significant contributor to their death.

2.1.2 Blood Supply to the Liver

The blood supply to the liver is a unique feature. Blood enters the liver through the hepatic portal vein and the hepatic artery. Approximately 75% of the liver's blood supply is received from the hepatic portal vein. This vein carries largely deoxygenated blood that has traveled from the heart to the digestive tract and major abdominal organs before entering the liver. The hepatic artery carries richly oxygenated blood directly to the liver to mingle with the deoxygenated venous blood and provide the remaining 25% of the blood supply. Once blood has entered the liver it travels through the sinusoids to the terminal hepatic venule (the central vein). The sinusoids are composed of incomplete endothelial walls and run in close contact with the hepatocytes (Sjaastad et al. 2003). This close proximity enables transference of small and large molecules, such as proteins,

between blood and cells. Blood exits the liver through the central vein which empties into the sublobular veins (Ross and Pawlina 2006).

2.1.3 Inflammatory Cells: Defenders of the Liver

2.1.3.1 Kupffer Cells

Kupffer cells are specialized hepatic macrophages of the mononuclear phagocytotic system (Ross and Pawlina 2006). They are located in the area lining the sinuosoids known as the Space of Disse (Shoelson et al. 2006). These cells are part of a first line of defense as harmful substances enter the liver through the portal blood vessels. They have the ability to secrete mediators of the inflammatory response, such as tumor necrosis factor alpha (TNF-α) and interleukins, thereby controlling the early phase of liver inflammation and playing a large role in innate immune defense (Roberts et al. 2007). Increased fat accumulation, oxidative stress, and proinflammatory cytokines, which participate in the development of insulin resistance in the liver, activate Kupffer cells (Reeves and Friedman 2002; Day 2006). Increased Kupffer cell activation and inflammatory gene expression in the liver due to fat accumulation during fasting may play a role in liver damage in fatty liver disease progression in mink. One way this may be accomplished is through interaction with hepatic stellate cells.

2.1.3.2 Hepatic Stellate Cells

Hepatic stellate cells are non-parenchymal cells located in the Space of Disse that normally store Vitamin A and lipids. They are activated by TNF-α which is secreted by activated Kupffer cells in response to certain pathological conditions such as chronic exposure to toxins including excessive lipid accumulation in non-lipid storing cells. Once activated, stellate cells convert into cells with myofibroblast characteristics (Ross

and Pawlina 2006). They are then unable to perform their storage responsibilities, instead synthesizing and depositing collagen into the peri-sinusoidal space (Reeves and Friedman 2002). Continued deposition of collagen results in liver fibrosis, most noticeably peri-portal and surrounding the central vein. During recovery and re-genesis hepatic stellate cells are involved in reforming the extracellular matrix (Ross and Pawlina 2006). Fibrosis is a common feature of the progression from simple fatty liver to steatohepatitis in humans (Brunt et al. 1999) but it is not known whether fatty liver disease progresses to steatohepatitis in mink.

2.2 Fatty Liver Disease

Fatty liver disease, also called non-alcoholic fatty liver disease (NAFLD) in humans, is an umbrella term that has been further divided into a two hit hypothesis (Day and James 1998; Day 2002). The first hit is fat accumulation. This is also known as hepatic lipidosis, or hepatic steatosis. It is characterized by accumulation of fat within the hepatocytes with some inflammation present (Cullen et al. 2006). While this condition enlarges the hepatocytes, compresses the sinusoids and interferes with blood and oxygen delivery throughout the liver, it is often benign in humans (McCuskey et al. 2004). The second hit is characterized by fat oxidation and induction of the inflammatory response (Day 2002). This may lead to steatohepatitis. Steatohepatitis, also called non-alcoholic steatohepatitis (NASH) in humans, is characterized by inflammation, fibrosis, presence of Mallory-Denk bodies, and cell death in addition to the fatty accumulation in the hepatocytes (Clark et al. 2002; Burt et al. 1998). Steatosis, leading to fibrosis and cirrhosis of the liver is associated with portal hypertension and liver failure (Iredale 2007). Fatty liver is commonly found in people afflicted with

obesity, primarily visceral, and type-2 diabetes. It is considered to be the hepatic manifestation of insulin resistance and is characterized by an unfavourable n-3/n-6 polyunsaturated fatty acid ratio (Videla et al. 2004; Adams et al. 2005).

Identification and characterization of factors involved in fatty liver disease development in mink and other carnivores is a relatively new field of study (Nieminen et al. 2009; Rouvinen-Watt et al. 2010) and very little is known about the development of the more advanced stages of fatty liver disease including steatohepatitis, fibrosis, and cirrhosis.

2.3 Nursing Sickness and Fatty Liver Disease

Mink nursing sickness is one of the largest causes of morbidity, 2-15% (Clausen et al. 1992; Schneider et al. 1992), and premature death, as high as 8% (Clausen et al. 1992; Schneider et al. 1992), in adult mink females annually. The cause of nursing sickness has not been well understood, however, recent research into the disease mechanisms and pathophysiology indicate that it is associated with insulin resistance and shares similarities with type-2 diabetes in humans (Hynes and Rouvinen-Watt 2007ab; Rouvinen-Watt 2003). Fatty liver is commonly diagnosed post mortem in mink dams that have died of nursing sickness (Clausen et al. 1992). Fatty liver is also often a consequence of rapid body weight loss due to lack of appetite or management practices that include restricted feeding regimes (Hunter and Schneider 1996; Hunter and Barker 1996). Protein-calorie malnutrition, choline and vitamin B deficiency, feed of inferior quality, clinical obesity, and restricted feeding have been cited as possible causes (Damgaard et al. 1994; Bjornvad et al. 2004; Mustonen et al. 2005a). This is similar to cats, where fatty liver disease is often diagnosed in animals that have recently been

subjected to stressors including change in food or lifestyle (Armstrong and Blanchard 2009). Fatty liver disease has been experimentally induced in mink (Bjornvad et al. 2004; Mustonen et al. 2005a) and other mustelid species including the sable, *Martes zibellina* (Mustonen et al. 2006), and the European polecat, *Mustela putorius* (Nieminen et al. 2009). It is believed to occur through the same mechanism as in nursing sickness, by mobilization of body fat reserves to meet energy demands (Wamberg et al. 1992).

2.3.1 High Risk Periods for Fatty Liver Disease Development

Fatty liver syndrome is a potentially fatal condition to which mink are at risk several times over the production cycle. These are during autumnal fattening (Rouvinen and Kiiskinen 1989; Korhonen and Niemelä 1997), the period during which the mink deposits higher amounts of fat in the visceral adipose depots in preparation for winter and possible food scarcity, during flushing in preparation for breeding (Tauson 1984), and during high stress periods including at parturition, and during mid-late lactation when energy demands on dams are the greatest (Hunter and Schneider 1996). Recent research in mink suggests that a disruption in glucose homeostasis may occur in dams during gestation leading to insulin resistance (Hynes and Rouvinen-Watt 2007ab). This is similar to the degree of insulin resistance that occurs during fetal development and milk production in humans (Di Cianni et al. 2003). However, a period of fasting, which mink may undergo during high stress periods, aggravates this normal metabolic response resulting in the mobilization of body fat stores to the liver leading to lipidosis (Bjornvad et al. 2004; Mustonen et al. 2005b), induction of an imbalance in the n-3/n-6 ratio (Nieminen et al. 2006) similar to that seen in humans, and may increase oxidative stress as seen in humans (Videla et al. 2004). These changes may be significant contributing

factors to the development of nursing sickness and the associated fatty liver disease in the mink (Rouvinen-Watt 2003) and may lead to progression to steatohepatitis similar to the human non-alcoholic steatohepatitis (NASH).

2.3.2 Disease Signs and Pathophysiology

The signs of mink nursing sickness are similar to those seen in cats with idiopathic feline hepatic lipidosis. These include weight loss, depression, anorexia, and dehydration (Schneider and Hunter 1992; Cornelius and Jacobs 1989; Griffin 2000). Ferrets with diabetes mellitus also show fatty liver development and display similar signs to the cat and mink including inappetance, rapid weight loss, dehydration, and hyperglycemia (Carpenter and Novilla 1977; Benoit-Biancamano et al. 2005). Upon necropsy, the livers of animals suffering from fatty liver appear greasy in texture, yellow in color, and enlarged (Burt 2001, Mustonen et al. 2005b).

Previous research in mink and other members of the *Mustelid* family has shown that fatty liver can develop within 2-7 days in response to fasting (Nieminen et al. 2009; Bjornvad et al. 2004; Mustonen et al. 2005ab; 2006; Nieminen et al. 2006). This is much sooner than in cats where studies have shown that hepatic lipidosis occurs when fasted for 14 days (Griffin 2000). Previous fasting experiments in mink have shown that significant weight loss occurs between 2-7 days (Mustonen at al. 2005ab) and similarly 6-10 days (Bjornvad et al. 2004). However, liver weight increases over the same time period (Mustonen et al. 2005ab; Bjornvad et al. 2004) indicating lipid accumulation in the liver as a result of mobilization of body fat reserves (Damgaard et al. 1998). Liver weight has been shown to increase in fasted domestic cats and biopsy sections often float in water or formalin (Griffin 2000). Normal mink liver contains between 2-4% lipids

(Damgaard et al. 1994). This can increase to between 25-34 % in mink diagnosed with fatty liver (Damgaard et al. 1994). Diagnosis of non-alcoholic fatty liver disease (NAFLD) in humans is usually done using routine histological staining and a grading scheme (Brunt et al. 1999). Diagnosis of steatohepatitis in humans usually includes identification of Mallory-Denk bodies (MDBs) in histological specimens. MDBs are considered the hallmarks in many liver diseases including NASH. MDBs can be visualized using routine histological stains including hematoxylin and eosin (H&E) and Masson's Trichrome (Brunt et al. 1999; Kleiner et al. 2005; Merat et al. 2010). To date, Mallory-Denk bodies have not been identified in mink but they could be indicators of disease progression in the mink liver due to fasting-induced fatty liver.

2.4 Histological Confirmation and Evaluation of Fatty Liver Disease

The gold standard for confirming the presence of fatty liver is still through histological assessment of a liver biopsy (Adams et al. 2005; Merat et al. 2010). Sampling variation and between observer reliability are concerns when interpreting liver biopsy results as the most commonly used methods of evaluation are considered somewhat subjective (Angulo 2007; Hübscher 2006). The method devised by Brunt et al. (1999) is considered effective for scoring non-alcoholic steatohepatitis (NASH) relating to liver damage and repair (Scheuer and Lefkowitch 2000). According to this method liver samples are categorized by grading and staging, rather than each being given a numerical value, as this has been found to increase the reproducibility of the evaluation between observers (Brunt et al. 1999). The grading component indicates ongoing hepatocyte damage whereas staging is meant to measure overall progressive liver injury which is evidenced by the presence and extent of fibrosis and cirrhosis (Hübscher 2006).

The downfall of this method is that it fails to include a component of liver injury that has since been deemed important in the development of fatty liver disease; portal inflammation (Merat et al. 2010). In 2005, Kleiner et al. proposed a new method based on the Brunt et al. (1999) method which was used to differentiate NASH versus not NASH. However it did not include a numerical component to measure disease progression and severity. Merat et al. (2010) have since devised a system which takes into consideration the downfalls of both previously mentioned methods. In this system the non-alcoholic steatohepatitis activity index (NAI) is used to determine the presence and severity of non alcoholic fatty liver disease (the grade). The four variables measured by the NAI are: steatosis, hepatocyte ballooning, lobular inflammation, and portal inflammation. The NAI gives an indication of hepatocyte damage and presence of the inflammatory response. This scoring system also analyzes non alcoholic steatohepatitis (stage) in the same manner as the Brunt et al. (1999) method. The presence of fibrosis indicates risk of disease progression from simple fatty accumulation to more severe and potentially irreversible liver pathology which can progress to cirrhosis and then liver necrosis. This scoring method developed by Merat et al. (2010) assigns values for the grade and stage of disease progression which allows for quantitative analysis of the results.

Steatohepatitis has not been reported in mustelids to date. The previously mentioned methods of evaluating NAFLD and NASH could be used to identify the presence of and quantify the severity of fatty liver disease and steatohepatitis in the American mink.

2.4.1 Types of Steatosis: Macrovesicular and Microvesicular

Two types of fat accumulation are seen in fatty liver disease biopsies; macrovesicular and microvesicular. They are often seen together as NAI score increases (Merat et al. 2010). Hepatocytes afflicted with macrovesicular steatosis are characterized by large lipid vacuoles that occupy the greater part of the hepatocyte, displacing the nucleus and cytoplasm to the periphery of the cell (Scheuer and Lefkowitch 2000). Microvesicular steatosis is characterized by finely divided fat accumulation in hepatocytes with the nucleus remaining central to the cell (Scheuer and Lefkowitch, 2000). Microvesicular steatosis is considered to be much more serious than macrovesicular as the accumulation of fat in this condition is thought to be most often a result of mitochondrial damage which leads to impaired beta oxidation of free fatty acids (Adams et al. 2005; Burt 2001), which in turn leads to endoplasmic reticulum stress and induction of the unfolded protein response. Neither mitochondrial damage nor microvesicular steatosis has been reported to date in mink liver exposed to short term fasting.

2.4.2 Non-alcoholic Steatohepatitis Activity Index (Grading)

Hepatocellular steatosis, ballooning and disarray of hepatocytes, and inflammation, characterized by the infiltration and identification of inflammatory cells, are all considered when grading liver biopsies (Brunt et al. 1999; Hübscher 2006; Merat et. al 2010). An NAI of 0 indicates that lipid accumulation is present in less than 5% of the lobule (Merat et. al 2010). According to the Merat et al. (2010) method, in humans, an NAI of mild (1-4) indicates that lipid infiltration, predominantly macrovesicular, is mostly present in acinar zone 3, minimal hepatocyte ballooning is present, there is mild

or no portal inflammation, 1-2 foci of neutrophils with some scattered neutrophiles within the lobule, and less than 1/3 of the lobule is affected. An NAI of moderate (5-8) indicates that lipid infiltration is present in acinar zone 3 and into 2, obvious hepatocyte ballooning and disarray can be observed, lobular inflammation is more noticeable with more than 2 neutrophil foci present, portal inflammation is nearly always present, and approximately 2/3 of the lobule is affected. An NAI of severe (9-12) indicates that lipid infiltration is present in all three acinar zones. It is characterized by obvious hepatocyte ballooning, disarray, lobular inflammation may progress to a chronic level with more than 4 neutrophil foci per 20x objective, and portal inflammation may be severe.

2.4.3 Staging

Livers are staged to indicate presence and severity of fibrosis in the liver tissue. Scoring of this aspect of fatty liver disease is done in humans to monitor the progression of NASH to indicate when liver failure might occur. Fibrosis occurs as an outcome of activation of the hepatic stellate cells which produce and deposit collagen into the peri-sinusoidal space in response to activation by Kupffer cells. Merat et al. (2010) have reported that initial deposition of collagen (fibrosis) commonly occurs in the peri-venular and peri-sinusoidal areas. As the disease condition increases in severity the fibrosis extends to the peri-portal area. It then progresses between portal areas to form collagen/fibrotic bridges (Brunt et al. 1999; Merat et al. 2010). Finally cirrhosis and liver necrosis occurs. In humans it has been reported that once a patient develops NASH the disease progresses to liver cirrhosis in 15-20% of cases (Tilg 2010). This irreversible damage has not been observed in mink suffering from fasting induced fatty liver disease.

However, the progression from simple fatty liver to steatohepatitis has not yet been studied.

2.5 Mallory-Denk Bodies

Another unexplored area in relation to fatty liver disease in mink is the presence of Mallory-Denk bodies. Mallory bodies were first identified and linked to alcohol abuse by Dr. Frank B. Mallory in 1911. The name was modified to Mallory-Denk bodies (MDBs) in 2007 in deference to Dr. Helmut Denk who, along with his collegues, described the first animal model of Mallory bodies in 1975 (Zatloukal et al. 2007). Since that time these inclusion bodies, or aggresomes, have been shown to form not only in human alcoholic steatohepatitis, NASH, and chronic cholestatic liver disorders (Zatloukal et al. 2004ab; Denk et al. 2000; Omary et al. 2002) but also in many neurodegenerative diseases including Alzheimer's, Parkinson's, and Huntington's diseases (Taylor 2002).

2.5.1 Mallory-Denk Body Composition

An aggresome has been defined as "a peri-centriolar, membrane-free, cytoplasmic inclusion containing misfolded, ubiquinated proteins ensheeted in a cage of intermediate filaments formed specifically at the microtubule organization center" (Johnston et al. 1998). MDBs are primarily composed of a cage of two intermediate filament proteins of hepatocytes, polypeptides 8 and 18 (Denk et al. 2000; Omary et al. 2002). These are 58kD and 45kD proteins respectively (Chamulitrat et al. 2007). It is theorized that MDB formation is a result of hyperphosphorylation of cytokeratins (Yuan et al. 1998) followed by ubiquination and inclusion of proteasomes from the ubiquitin-proteasome pathway which is also seen in aggresome formation (Johnston et al. 1998; Anton et al. 1999; Wigley et al. 1999). This theory is supported by a study conducted by Bardag-Gorce et

al. (2001) in which antibodies to the proteasomal subunits and to ubiquitin colocalized at the edges of the MDBs when viewed under confocal microscopy.

2.5.2 Mallory-Denk Body Formation and Endoplasmic Reticulum Stress

There are many theories regarding the triggers by which MDBs are formed. A study by Hanada et al. (2007) suggests that endoplasmic reticulum (ER) stress plays a role in MDB formation in liver disease.

The ER is the peri-nuclear cytoplasmic organelle where proteins and lipids are synthesized (Lee 2005). It is responsible for the proper folding and delivery of various proteins to the secretory pathway (Kostova and Wolf 2003). Unfolded proteins are properly folded into their tertiary structures in the lumen of the ER with the aid of various protein chaperones and are then transported to the Golgi apparatus before being secreted from the cell (Ellgaard et al. 1999).

Accumulation of lipids in the ER, as in fatty liver disease, interrupts cellular homeostasis and impairs cell function. Normally the cell metabolizes lipids by mitochondrial oxidation or lipoprotein secretion. However in situations where excess lipids are accumulating in the ER, oxidative stress increases because the cell is unable to dispose of lipids via lipoprotein secretion and fatty acid oxidation as quickly as lipid uptake and biosynthesis occurs (Abdel-Malek and Diehl 2006). Oxidative stress leading to the production of reactive oxygen species (ROS) has been shown to have negative effects on ER function resulting in an increase in misfolded proteins in the ER lumen and in MDB-like inclusion formation in cultured cells (Hanada et al. 2007). Based on immunofluorescence analysis, Hanada et al. (2007) found that inclusion bodies from cultured hepatocytes shared similar morphologic characteristics with MDBs. In both

cases myelin-like deposits were found in the mitochondria of inclusion containing cells and both were composed of intermediate filaments although the cell-cultured MDBs did not completely resemble typical MDBs. The scientists hypothesized that this could be due to differing stimulation times.

2.6 Endoplasmic Reticulum Defense Mechanisms

There are two main systems to degrade the intracellular components of a eukaryotic cell: the unfolded protein response and lysosomal degradation via autophagy (Cuervo 2004). When unfolded proteins begin to accumulate in the ER lumen the internal defense response, the unfolded protein response (UPR), is activated (Sitia and Braakman 2003). Research conducted on yeast by Travers et al. (2000) suggests that the purpose of the activated UPR is to modify the action of the protein secretory pathway in order to minimize the amount and concentration of unfolded proteins in the ER thereby reducing ER stress. Autophagy is the last line of defense to dispose of misfolded proteins after the UPR has become overwhelmed. Activation of the UPR in response to ER stress is a key feature in the development of insulin resistance in humans (Özcan et al. 2004) and may be significant to our understanding of the development of fatty liver and possible steatohepatitis in the mink.

2.6.1 The Unfolded Protein Response

The UPR is the mechanism by which ER stress is alleviated through the activation, transcriptional up-regulation, and action of various molecular chaperones and enzymes and the repression of further protein translation within the ER (Mori 2000). Chaperones and enzymes are responsible for refolding misfolded proteins and also for aiding in the degradation of misfolded proteins that cannot be refolded properly. One

such chaperone is glucose regulated protein 78 (GRP78), also known as immunoglobulin binding protein (BiP). GRP78 has frequently been used as a general indicator of ER stress and subsequent induction of the UPR (Lee 2001) and may be a useful indicator of oxidative stress leading to ER stress in the mink.

2.6.2 Glucose Regulated Protein 78 Messenger Ribonucleic Acid and Protein Expression

Glucose regulated protein 78 (GRP78), a 78kD member of the heat shock protein family, is one of the best characterized ER resident molecular chaperones in humans (Chamulitrat et al. 2007). Its synthesis is stimulated by a variety of physiological and environmental conditions, such as glucose deprivation, accumulation of unfolded proteins, intracellular calcium efflux, and other pathological conditions, which result in disruption of normal ER function and homeostasis (Lee 2005). GRP78 facilitates proper protein folding, and prevention of protein aggregate formation. It also functions to prevent cell apoptosis when the ER is under stress by interfering with caspase activation (Reddy et al. 2002).

In situations where high volumes of unfolded proteins are accumulating in the ER, GRP78 may play a role in translational attenuation of protein synthesis (Bonificino and Weissman 1998), as it is directly involved in the activation of protein kinase RNA-like endoplasmic reticulum kinase (PERK) in response to ER stress (Bertolotti et al. 2000). In a normal non-stressed cell GRP78 binds to the ER transmembrane proteins PERK and activating transcription factor 6 (ATF6) and maintains them in an inactive state. Upon the induction of ER stress these transducers are released from GRP78 and become activated to carry out specific functions in the cell (Bertolotti et al. 2000; Hong et al. 2004). Harding et al. (2000) have shown that PERK is integral to the attenuation of

protein translation in response to ER stress in a study of mouse embryonic stem cells. Upon its release and activation, ATF6 acts as an active transcription factor for the UPR target genes including GRP78 (Hong et al. 2004). In situations where cells are deprived of glucose, such as in conditions of insulin resistance, synthesis of GRP78 has also been shown to increase (Lee 2005).

2.6.3 The Ubiquitin-Proteasome System

Oxidative stress and ROS production leads to accumulation of unfolded proteins within the ER lumen, hepatocellular dysregulation, and activation of the UPR. Once the UPR is activated unfolded proteins that cannot be refolded properly are removed from the ER and degraded by the ubiquitin-proteasome system (UPS) to prevent them from cluttering up the cell, causing further cellular dysfunction, and forming MDBs. Abnormal folding of proteins exposes the hydrophobic residues which would normally be located inside of the properly folded protein (Kopito 2000). In response to the exposure of the residues the cell activates the chaperone system to promote refolding and the proteasome system for the removal of proteins that cannot be refolded. Some proteins cannot be re-folded properly because of their morphology (Michalik and Van Broeckhoven 2003). Such features as misreading of the protein code leading to placement of an incorrect amino acid into the protein chain sequence leads to the inability of the cell to fold the protein properly. Proteins that cannot be refolded by chaperones are degraded in the cytoplasm via the intracellular proteasomal system (Rock et al. 1994).

Normally misfolded proteins that are tagged for degradation are marked by ubiquination in order to be transferred to the proteasome complex. Upon arrival the protein is de-ubiquinated and enters the 26S proteasome complex for degradation. The

complex is composed of a 20S central hollow cylinder, the cavity of which is the site of degradation, tapering at either end to limit entering substrates to short peptides and completely unfolded proteins (Coux et al. 1996). Once proteins aggregate they are very stable and must first be separated into individual unfolded proteins and de-ubiquinated before they will fit properly into the proteasome complex for degradation. This becomes increasingly difficult as proteins continue to aggregate and does not always occur leading to blockages in the proteasome complex rendering it incapable of further protein proteolysis (Kisselev et al. 2002).

Using immunohistochemical analysis of MDB formation in a drug primed mouse model, Bardag-Gorce et al. (2001) observed that there are reduced numbers of proteasomes in cells containing MDBs. They hypothesized that the reduction of proteasomes in these cells led to increases in the number of ubiquinated proteins favoring cytokeratin aggregation. Further study by Bardag-Gorce et al. (2002) led to the hypothesis that the absolute number of proteasomes does not decrease but that covalent bonding between ubiquitinated protein complexes and proteasomes occurs which means that the number of functional proteasomes in the cell decreases. These complexes are thought to bind to the accumulating cytokeratins contributing further to decreased numbers of functional proteasomes in the cell and reducing elimination of accumulating cytokeratins. This same study showed that co-localization of ubiquitin and proteasomes occurs in MDBs. Harada et al. (2003) reported that inhibition of proteasome action of the UPS induces intermediate filament inclusions and causes the Golgi apparatus to function improperly leading to cellular dysfunction. A study by Bence et al. (2001) found that

aggregation of proteins leads to impairment of proteasome function which ultimately results in impairment in cellular function.

Research by Hanada et al. (2007) suggests that there is a link between oxidative stress and reactive oxygen species (ROS) production in the ER and MDB formation in liver disease. They found that treating cultured human hepatoma (Huh7) cells with a combination of glucose oxidase (GO) and acetyl-leucyl-leucyl-norleucinal (ALLN) induced oxidative stress and ROS production and resulted in MDB formation. Treatment with the antioxidant *N*-acetyl-cysteine (NAC) inhibited inclusion body formation indicating that oxidative stress and ROS are associated with MDB formation in human liver cells *in vitro* (Hanada et al. 2007). They suggest that MDB formation occurs as an outcome of dysfunction of the ER in response to oxidative stress resulting in an increase of mis-folded proteins, failure of the ubiquitin-proteasome protein degradation system, and failure of cellular autophagy. It is not known what effect, if any, fat accumulation and ER stress have on development of MDBs and steatohepatitis in mink.

2.6.4 Autophagy

Autophagy is the process responsible for the degradation of cytoplasmic proteins and organelles into their fundamental components using lysosomal enzymes (Cuervo 2004; Harada et al. 2008). The role of autophagy, not just in apoptosis but also in cellular defense and housekeeping, has recently become a focus in the study of many human disease processes (Cuervo 2004). As misfolded proteins continue to accumulate and form MDBs, trapping proteasomes and chaperones within them, they become resistant to removal through the action of the UPS. When this occurs, removal by autophagy, through the action of lysosomes, is the only possibility (Michalik and Broeckhoven

2003). When proteins are just beginning to aggregate into MDBs they can be removed by autophagy, however as the disease progresses and numbers and size increase they become less susceptible to degradation by lysosomal enzymes. Autophagy has the ability to protect cells from death so long as the damage can be healed. However, a prolonged UPR will eventually lead to cell exhaustion and cell death, or apoptosis (Webb et al. 2003; Ravikumar et al. 2002).

2.6.5 Apoptosis

Apoptosis, also known as programmed cell death (PCD), is thought to be activated by autophagy when cellular damage is irreversible, however, the mechanism by which this is accomplished is not well understood to date (Kurz et al. 2008). As liver cells die they are replaced with fibrous tissue leading to cirrhosis and liver disease. Progressive liver disease leads to liver failure and death of the organism as the liver can no longer support numerous essential biochemical pathways in the body. However, there is evidence that liver recovery can occur if the stressors are resolved or removed and the UPR is relieved. Mouse models suggest that elimination of MDBs and return to normal hepatocellular keratin network occurs within four weeks of recovery after removal of a drug that induces liver disease (Denk and Eckerstorfer 1977; Zatloukal et al. 1990; Zatloukal et al. 2004ab).

CHAPTER 3.0: OBJECTIVES AND HYPOTHESIS

The overall objectives of this research are to characterize the time course of development of fasting-induced steatohepatitis in the mink using Mallory-Denk bodies (MDBs) and glucose regulated protein78 (GRP78) messenger ribonucleic acid (mRNA) as indicators of endoplasmic reticulum stress, and induction of the unfolded protein response. Characterization of liver recovery to the pre-fasted state from the changes that occurred during lipid accumulation by studying MDB elimination and GRP78 mRNA levels after a four week re-feeding period post 7-d fast was a second objective.

It is hypothesized that fasting will promote the progression of simple steatosis to the more severe and life threatening steatohepatitis and will be characterized by the formation of MDBs, liver fibrosis, and increased levels of the protein molecular chaperone GRP78 as has previously been reported in humans and other species.

CHAPTER 4.0: MATERIALS AND METHODS

4.1 Animal Experiment

Sixty (n = 60) 9 month old mink of the standard black color type, five males and five females per experimental group, were fasted for 0, 1, 3, 5, or 7 days to study the effects of fasting on the development of fatty liver disease in mink. In addition, one group was fasted for 7 days followed by a period of re-feeding (RF) for 28 days to study recovery from disease pathophysiology.

Mink were fed a standard commercial diet as reported in Rouvinen-Watt et al. (2010) prior to fasting and during the re-feeding portion of the experiment. Water was provided *ad libitum* to all groups throughout the duration of the experiment. The study ran from January 9 – February 13, 2007. Fasting of the animals occurred from January 10 to January 16, 2007. The RF group was re-fed from January 16 to February 13, 2007. The mink were housed individually in standard sized pens with a nest box containing aspen bedding at the Canadian Centre for Fur Animal Research located at the Nova Scotia Agricultural College, Truro, Nova Scotia, Canada.

The mink were housed in a separate building isolated from the main herd during the fasting regimes to alleviate the potential stress that could result from the normal feeding practices for the non-experimental mink. The mink were evaluated daily by the unit staff and on days 0, 1, 3, 5, and 7 of the trial by research team members and two licensed veterinarians to ensure that all were fit to continue their respective fasting regimes. There were no cases of morbidity or mortality over the course of this experiment; however, two female mink in the RF group were euthanized and sampled on day 6 of the fasting regime due to the loss of greater than 20% body weight (BW). The

remainder of the female mink in the RF group were re-fed on day 6 rather than day 7 for the same reason; rapid body weight loss. All procedures carried out over the course of the experiment were approved by the Animal Care and Use Committee of the Nova Scotia Agricultural College and were carried out in accordance with the guidelines of the Canadian Council for Animal Care.

4.2 Euthanasia and Sample Collection

All animals were weighed to the nearest gram prior to the onset of fasting as well as prior to the onset of re-feeding. At the end of each experimental regime the mink were weighed to the nearest gram, anaesthetized (dosages: 3.4 mg/kg BW of xylazine, 8.5 mg/kg BW of ketamine which equal: 0.17 ml/kg BW of Rompun® [xylazine 20 mg/ml] and 0.09 ml/kg BW of Ketalean® [ketamine hydrochloride 100 mg/ml]), sampled for blood, and euthanized by intra cardiac injection of Euthanyl® (pentobarbital 240 mg/ml, 0.44 ml/kg BW). Prior to euthanasia mink were subjected to a 12 hour fast by staggering removal of feed according to the sampling schedule to ensure an empty digestive tract for cleaner sampling.

The livers were dissected and the gallbladder removed before being weighed with a precision of ±0.01 g. They were then divided into five sections; one small section (2 g or less) from the left median lobe was placed in 10% buffered formalin to be processed for histology and stained using haematoxylin and eosin and Masson's Trichrome to evaluate liver pathology over the fasting and re-feeding periods. Two sections each weighing between 2-5 g were placed in two separate cryovials which were then snap frozen in liquid nitrogen and stored at -80°C. These were designated for quantitative real time polymerase chain reaction (qRT-PCR) analysis, one of which was used for analysis

of GRP78 mRNA levels. The first of the two remaining liver tissue samples was placed into a sample bag and snap frozen in liquid nitrogen and then stored in -80°C for the analysis of total lipid content according to Folch et al. (1957). The remainder of the left median lobe, the second of the remaining liver tissue samples, was snap frozen in liquid nitrogen and stored at - 80°C. This study involved Masson's Trichrome staining and GRP78 mRNA quantification using qRT-PCR.

4.3 Histology: Masson's Trichrome Staining

Liver tissue samples, stored in 10% buffered formalin, were sent to the Hancock Veterinary Services at the Nova Scotia Agricultural College, Truro, Nova Scotia, Canada to be embedded in paraffin blocks, sectioned, and mounted on Superfrost Plus Microscope Slides (Fisher Scientific, Ottowa, Ontario, Canada). Slides were then transported to the Histology Laboratory at the Atlantic Veterinary College, Prince Edward Island, Charlottetown, Canada to be stained for Masson's Trichrome according to Luna (1968). The procedure followed is outlined in Table 1.

Slides were coverslipped and sealed using the automatic coverslipper (Tissue Tek Automatic Coverslipper, Somagen, Miles/Sakura, Japan). Slides were allowed to dry in a fumehood for 10 – 20 minutes before being transferred to slide boxes for storage until they could be visualized and analyzed via light microscope (Leica DM 500 microscope, Leica ICC50 camera; Leica Microsystems, Ontario, Canada) for grade of fatty liver development and stage of fibrosis.

4.3.1 Histological Assessment of Steatosis and Fibrosis

Slides were evaluated according to the method proposed by Merat et al. (2010), a modification of the benchmark protocol designed by Brunt et al. (1999), and the method

by Kleiner et al. (2005). One slide per animal was examined. The entire slide was imaged by taking sequential pictures and a representative field of view was chosen for the determination of the NAI score. Thirty days after the first evaluation, a second evaluation was performed by the same person and the average of the two scores was used for statistical analysis. In order to eliminate bias, the slides were numbered from 1-60 with no knowledge of the group or the sex of the mink at the time of the evaluation.

The non-alcoholic steatohepatitis activity index (NAI) proposed by Merat et al. (2010) was used to determine the presence and severity of non alcoholic fatty liver disease (the grade). This scoring system also analyzes non alcoholic steatohepatitis (the stage) as evidenced by the presence and severity of fibrosis within the tissue. The presence of fibrosis indicates risk of disease progression from simple fatty accumulation to more severe and potentially irreversible liver pathology which can progress to cirrhosis and then liver necrosis. The NAI (grade) represents the degree of fatty accumulation and progression of NAFLD. It is comprised of the sum of four histologic features: Steatosis, hepatocyte ballooning, lobular inflammation, and portal inflammation (Table 2). NAI of 0 indicates normal liver architecture and no NAFLD present. NAI of 1-4 indicates mild NAFLD, 5-8 indicates moderate, and 9-12 indicates severe NAFLD histopathology.

Stage indicates the progression of fibrosis where NASH is present (Table 2). A stage score of 0 indicates that no steatohepatitis is present. A score of 1 indicates that the initial phase of fibrosis in NASH has begun. Fibrosis typically begins in acinar zone 3 in the peri-venular and peri-sinusoidal areas (Brunt et al. 1999). A score of 2 indicates that fibrosis has progressed from the peri-venular and peri-sinusoidal areas to the periportal areas. A score of 3 is applied when fibrosis extends from the peri-venular, peri-

sinusoidal, and peri-portal areas to include bridging fibrosis between portal areas, joining them together. A score of 4 indicates that the liver has become cirrhotic. This means that liver cells are undergoing apoptosis and widespread liver death is occurring.

Slides were graded using the 25x objective and staged using the 25x and 40x objectives. Reference images used were from Merat et al. (2010) and Brunt et al. (1999).

Table 1. Masson's Trichrome procedure.

Procedure	Time
Deparaffin and dehydrate slides to distilled water:	
Xylene	10 minutes
Absolute Alcohol	2 minutes
95% Alcohol	2 minutes
70% Alcohol	2 minutes
Distilled water	2 minutes
Mordant in Bouin's Solution	1 hour
Placing slide holder into glass dish and run tap water into dish until water runs clear	10 minutes
Rinse slides under running distilled water	1-2 minutes
Stain hepatocyte nuclei black: Place slides into Weigert's iron hematoxylin solution	10 minutes
Placing slide holder into glass dish and run tap water into dish until water runs clear	10 minutes
Rinse slides under running distilled water	1-2 minutes
Place slide holder into Biebrich Scarlet-acid fuschin solution	4 minutes
Rinse slides individually under running distilled water until water runs clear	30 seconds
Place slide holder into phosphomolybdic-phosphotungstic acid	12 minutes
Place slide holder into Aniline blue solution	5 minutes
Rinse slides individually thoroughly under running distilled water	30 seconds
Place slide holder into 1% glacial acetic acid	4 minutes
Dehydrate and clear slides:	
95% Alcohol (fresh)	2 minutes
Absolute alcohol	2 minutes
Xylene	10 minutes

Table 2. NAI and NASH scoring system as proposed by Merat et al. (2010) used to evaluate mink liver.

Variable	Score	Description
A. Steatosis	0	None
	1	Up to 33% of acini, mainly macrovesicular
	2	34-66% of acini, commonly mixed steatosis
	3	Over 66% of acini (panacinar), commonly mixed steatosis
B. Hepatocyte ballooning	0	None
	1	Occasional in zone III
	2	Obvious in zone III
	3	Marked, predominantly in zone III
C. Lobular inflammation	0	None
	1	Scattered neutrophils, occasional mononuclear cells, 1 or 2 foci per 25x objective
	2	Neutrophils associated with ballooned hepatocytes, mild chronic inflammation, 3 or 4 foci per 25x objective
	3	Acute and chronic inflammation, neutrophils may concentrate in zone III, over 4 foci per 25x objective
D. Portal inflammation	0	None
	1	Mild, some portal areas
	2	Mild to moderate, most portal areas
	3	Moderate to severe, most portal areas
E. Stage	0	No fibrosis
	1	Zone III peri-venular peri-sinusoidal (peri-cellular) fibrosis
	2	Stage I changes + peri-portal fibrosis
	3	Bridging fibrosis
	4	Cirrhosis
		NAI (Sum: A-D): Stage (E):

4.4 Detection and Quantification of Glucose Regulated Protein, 78kDA (GRP78) Messenger Ribonucleic Acid Using Quantitative Real Time Polymerase Chain Reaction: Assay Development

Quantitative real time polymerase chain reaction (qRT-PCR) was performed to compare liver GRP78 messenger ribonucleic acid (mRNA) expression levels, an indicator of endoplasmic reticulum stress, between groups of mink fasted from 0 to 7 days. Messenger ribonucleic acid levels were also compared between the fasted groups and one group of mink that was first fasted for 7 days and then re-fed for a period of 28 days prior to euthanasia. A two-step qRT-PCR assay was performed; the reverse transcription to obtain complementary deoxyribonucleic acid (cDNA) and the real time PCR assay were completed in two separate reactions rather than combined into one reaction (Wong and Medrano 2005). Ribonucleic acid was first isolated (extracted) from the liver tissue and characterized to determine the quantity obtained and the quality or integrity of the product. Next, complementary deoxyribonucleic acid (cDNA) was synthesized from the RNA for use as the polymerase chain reaction (PCR) template. The PCR reaction generated raw fluorescence data which was then adjusted to the baseline and manipulated to generate the output dataset containing GRP78 mRNA gene expression levels which, once normalized, were statistically analyzed for significant differences between treatment groups. In order to normalize the qRT-PCR results a ratio was calculated using a housekeeping gene (HKG). Two HKGs were tested: 18S ribosomal RNA (rRNA) and glyceraldehyde-3-phosphate dehydrogenase (GAPDH). Results are thus expressed as GRP78 mRNA/HKG ratio.

4.4.1 Ribonucleic Acid Isolation

Total RNA content was extracted from up to 30 mg of liver tissue per sample using the RNeasy® Mini Kit (Qiagen, Mississauga, Canada) following the manufacturer's instructions. First, the samples were homogenized and lysed in a guanidine thiocyanate denaturing buffer to inactivate RNases, the presence of which would degrade the RNA. Ethanol was then added to facilitate binding of RNA to the silica membrane in the spin column. The sample was transferred into the spin column, washed clean of contaminants using Buffer RW1, and spun three times using a microcentrifuge at 8871 g. The sample was incubated with DNase I for 15 minutes before washing with Buffer RW1. Pre-elution was accomplished using Buffer RPE and spinning for 15 seconds at 8871g. The RNA in the sample bound to the membrane while contaminants washed away. The RNA was then eluted in 30-100 µl of RNase free water. The concentration of the RNA was quantified by optical density at 260 nm using the Nanodrop ND1000 spectrophotometer (Thermo Fisher Scientific, Delaware, USA). The purity of the RNA was assessed by the ratio of the A260 / A280 readings (a ratio less than 1.8 may indicate protein contamination) and the ratio of the A260 / A230 readings (a ratio less than 1.8 may indicate salt or ethanol contamination). The quality of the RNA was determined by running the sample on 0.7% agarose gel. The presence of intact 28S and 18S ribosomal RNA bands, the 28S band being more intense, indicated the presence of good quality (undegraded) RNA.

4.4.2 Complementary Deoxyribonucleic Acid Synthesis

Reverse transcription of the extracted RNA using the High Capacity cDNA Reverse Transcription Kit with RNAse Inhibitor (Applied Biosystems, California, USA)

was performed to obtain complementary deoxyribonucleic acid (cDNA) for PCR using the manufacturer's instructions. A 2X master mix was prepared according to the manufacturers instructions and pipetted into 8-well tube strips containing 1.0µg total RNA in an equal volume. Each well was mixed gently using a pipette tip by drawing the solution up and down the tip twice. The plate was placed into the Dyad® Peltier Thermal Cycler (BIO-RAD, Mississagua, USA) and run at 25°C for 10 min., 37°C for 120 min., 85°C for 5 seconds, and held at 10°C to end the procedure. The cDNA produced was spun down and stored at -35°C. As needed, 10-fold and 100-fold dilutions of the cDNA were prepared in 10mM Tric-Cl, pH 7.4, and stored at -35ºC. The cDNA was stored in five randomized blocks but so that there would be one male and one female from each treatment group within each of the five blocks. Blocking was done in this way to reduce error due to day of sample processing.

4.4.3 Primer Design to Isolate Mink Specific Glucose Regulated Protein 78 Sequence

A search through GenBank revealed that mink specific sequence for the gene encoding GRP78 was not available. Therefore, forward and reverse primers using Primer 3 software were designed to sequence the target gene by comparing GenBank published GRP78 sequences from selected reference sequences in human (NM_005347), dog (XM_537847), and rat (NM_013083). The human sequence was then used as a template in a BLAST search for homologous sequences in the Genbank expressed sequence tags (cDNA) library from the Mustelidae, and the ferret sequence GD184947 was identified as homologous to the human gene. In order to design primers which would amplify mink GRP78, areas highly conserved between the above sequences, and the predicted giant panda (XM_002916311) GRP78 sequence were targeted as areas around which to design

primers (Table 3). The sequence was entered into Primer 3 software (Whitehead Institute for Biomedical Research, Massachusetts, USA) and primers designed from the homologous regions. Four sets of primer pairs were ordered. Initially, A and B (Table 3) pairs were tested. The primers were run with complementary cDNA (1µl) from obese mink liver as a template in a polymerase chain reaction (PCR) using the Dyad® Peltier Thermal Cycler (BIO-RAD, Mississauga, Ontario) to obtain mink PCR products which could be sequenced. The reaction mix was composed of: 1X PCR Buffer, 1.5mM $MgCl_2$, 0.2mM dNTP mix, 0.24uM of each Primer, 0.8U/ul Taq DNA Polymerase, and ddH_2O. Reaction conditions were: Incubate at 94°C for 5 min, incubate at 94°C for 30 seconds, gradient increase from 48°C-68°C in 30 seconds, incubate at 72°C for 1 min, cycle to step two 29 more times, incubate at 72°C for 6 min, incubate at 10°C and hold.

The PCR products were run on a 2% agarose gel to check that there was a single PCR product of the expected size and that no primer dimer or non specific binding was occurring. Primer dimer or non specific binding would show up in the form of an additional band(s) of inappropriate size(s). The first two primer pairs (A and B) did not yield sufficient PCR product for gel analysis. Therefore, the PCR product was column purified using the Montage™ PCR clean up kit (Millipore, Massachusetts, USA) and the purified products re-amplified as before using nested primer pairs (C and D) (Table 3), using the same conditions as previous (see above).

The products were again run on a 2% agarose gel and bands of the correct size were seen. Each PCR product was then column purified using the Montage™ PCR clean up kit (Millipore, Massachusetts, USA), quantified using the Nanodrop ND1000 spectrophotometer (Thermo Fisher Scientific, Delaware, USA), and then sent for

sequencing to the Atlantic Research Centre for Agricultural Genomics on the Nova Scotia Agricultural College campus, Nova Scotia, Canada. The sequence was then submitted to Genbank and accepted (Accession # HQ003898.1; Table 4).

The resulting mink specific sequence segments for GRP78 (Tables 5 and 6) were then aligned using the BioEdit (Ibis Therapeutics, California, USA) program, trimmed to remove unreliable sequencing run ends, and compiled into a consensus sequence. The consensus sequence was then compared to mammalian reference sequences using NCBI BLAST to confirm the identity as GRP78. The open reading frame (ORF) was identified using BioEdit and the resulting protein sequence was also compared to GRP78 protein sequences in other species.

4.4.4 Standards

The mink specific GRP78 sequence was entered into Primer 3 software (Whitehead Institute for Biomedical Research, Massachusetts, USA) to design T7 promoter primers for development of standards and to design qRT-PCR primers for quantification of GRP78 mRNA in mink liver samples. The primers designed by the software were entered in the National Center for Biotechnology Information (NCBI) primer BLAST (Maryland, USA) to compare to other mammalian gene sequences and ensure that there would be no non-specific binding occurring. The mink specific sequence was also evaluated using MFOLD (The RNA Institute, New York, USA) to check for hairpin structures in the sequence that might interfere with primer binding. Primers that overlapped hairpin structures were discarded as potential primers for this assay.

A PCR using the T7 promoter primers (Table 2) was performed on the Dyad® Peltier Thermal Cycler with obese mink cDNA using the same conditions as for primer pairs A and B (Table 2) to test the specificity of the T7 promoter primer pair. A 2% agarose gel was run using the PCR product to check for non-specific primer binding with the addition of guanosine to protect the DNA against degradation from UV and natural light (Gründemann and Schömig 1996). Gel purification was required as some non-specific binding occurred. The Wizard®SV Gel and PCR Clean-up System (Promega Corporation, Wisconsin, USA) was used to gel purify the band of the correct size. The purified T7 promotor tagged PCR product was then quantified using the Nanodrop ND1000 spectrophotometer and then used as the DNA template for *in vitro* transcription to produce copy RNA, which in turn was used to create standards for the qRT-PCR assay.

In vitro transcription was carried out on the T7 promotor tagged PCR product using the MEGAshortscript™ Kit (Applied Biosystems, California, USA) according to manufacturer's instructions. In brief, a 20µL solution containing 110nM template DNA, 1X Reaction Buffer, 7.5mM each ATP, CTP, GTP, and UTP, and 1X T7 Enzyme Mix was mixed in a 0.5ml microfuge tube and incubated in the Dyad® Peltier Thermal Cycler for 4 hours at 37°C. Then, 1µL of 2U/µL TURBO DNase was added to the reaction, mixed well, and the incubation continued at 37°C for an additional 15 minutes. The resulting copy RNA was purified using the RNeasy® Mini Kit (Qiagen, Mississauga, Canada). A 0.7% agarose gel for RNA was run to confirm size and purity of the product. Quantification was done using the Nanodrop ND1000 spectrophotometer.

Reverse transcription using the Applied Biosystems High Capacity cDNA Reverse Transcription Kit with RNase Inhibitor (California, USA) was performed on the copy RNA to produce a pure mRNA-like fragment of the gene of interest to be used for a qRT-PCR standard curve. The same procedure as described in section 4.5.2: Complementary DNA synthesis, above, was used. In order to minimize and standardize the effects of freeze-thaw cycles on the standards, the resulting cDNA was diluted to 1/10 using 10mM Tris Buffer, pH 7.6 and 10ul aliquots were transferred into each of 20 labeled low-binding tubes, frozen and stored at -30°C until needed. As required, one 1/10 dilution aliquot was removed from the freezer, thawed, diluted to 1/10, aliquotted and refrozen at -30°C as above, to make a 1/100 working stock. In this way error due to freeze thawing was further reduced.

4.4.5 Protocol Optimization

A five-fold dilution series using the 1/100 dilution standard was performed to determine primer activity for two sets of primers over a range of temperatures. The sensitivity of the assay was assessed using the standard curve and the efficiency of the assay was verified. The objective was to design an assay that yielded a single product of the appropriate size without primer dimer formation, which was assessed by the melt curve. The minimum criteria for a successful assay were a run efficiency higher than 1.8 (80%), with R^2 values over 0.97 (97%). The samples were run in triplicate, and the maximum acceptable coefficient of variation for the triplicates was 10%.

The primers chosen for mink GRP78 qRT-PCR are listed in Table 3. One tube of the GRP78 standard working stock 1/100 dilution was thawed and a 5-fold dilution series created using 10mM Tris-Cl, pH 7.4. Two mastermixes, identical except that each

contained a different primer pair, containing ddH_2O, 1X GoTaq Flexi Buffer, 2.5mM $MgCl_2$, 0.2mM dNTP mix, 0.1uM of each primer, 0.8U GoTaq HS DNA Polymerase (Promega), 1X EvaGreen® (Biotium), and 1µl cDNA were mixed. Each mastermix was divided into two tubes. Two of the nine 5-fold dilution GRP78 standard series tubes were selected, the second tube and the eighth tube, for testing. Each of the two GRP78 standard dilutions was added to one of the mastermix tubes to produce four combinations for testing. Twenty microliters from each mastermix was pipetted in triplicate into a PCR plate. The PCR was run on the BIO-RAD iQ5™ Multicolor Real-Time PCR Detection System using persistent run factors and an annealing temperature gradient from 54°C - 64°C. The run conditions were: One cycle at 95°C for 2 minutes, forty cycles at 95°C for 30 seconds followed by at temperature gradient from 54°C-64°C for 30 seconds, one cycle at 95°C for 10 seconds followed by 10 seconds at 65°C, and twenty-seven cycles from 70°C-96°C for 6 seconds to produce a melt curve. The same experiment was run using Ssofast™ EvaGreen® Supermix (Bio-Rad) rather than the GoTaq HS Polymerase mastermix to determine whether efficiency would increase. The master mix was composed of: ddH_2O, 1X SsoFast EvaGreen Mastermix (Bio-Rad), 0.5µM of each primer, and 1µl cDNA. Run conditions using the LightCycler®480 were: One cycle at 95°C for 30 seconds, and 45 cycles first at 95°C for 5 seconds followed by 58°C for 20 seconds. Finally, a melt curve was produced. Primer set F (Table 2) using the Ssofast™ EvaGreen® Supermix (Bio-Rad) and running at 57.9°C yielded the greatest efficiency.

4.4.6 Glucose Regulated Protein 78 Quantitative Real Time Polymerase Chain Reaction Assay

Quantification of mink liver GRP78 mRNA was performed using the Lightcycler®480 (Roche, Indianapolis, USA) at the Nova Scotia Agricultural College,

Truro, Nova Scotia, Canada. Samples were run using a 384-well plate so that that all could be run at once. Samples were randomized for treatment.

A 5-fold standard dilution series was run with the assay. This standard curve was used to generate a linear relationship between crossing point (C_p) and the initial amounts of cDNA. C_p and cycle threshold (C_t) are synonyms; C_p is used in LightCycler® (Roche Applied Science, Indianapolic, USA) literature and C_t is used in ABI PRISM® (Applied Biosystems, Foster City, CA, USA) literature. The crossing point (C_p) is the cycle number in the PCR reaction when the fluorescence intensity becomes greater than background fluorescence. The C_p, proportional to the number of copies of the DNA in the original template, along with the standard curve C_p produced using an external standard, allow the determination of the concentration of DNA in the unknown (target) samples (Heid et al. 1996).

To eliminate the possibility of accepting false positive results due to the non-sequence specific binding of DNA binding dyes a melt curve of the run was performed. The melt is the temperature at which the product double helix separates into single strands at the end of the amplification process. The machine increases the temperature by fractions of a degree until the product for each sample melts. Ideally all samples will melt at the same temperature. The machine then plots these onto a graph as melting peaks. The presence of PCR products of the incorrect size would be revealed by the melting peaks at a different temperature from the standards. Gel analysis was also used to determine the specificity of the PCR reaction. One clear band of the correct size (GRP78 = 662 bp) indicated that the product was specific.

A Ssofast™ EvaGreen® Supermix mastermix was prepared for the GRP78 assay. All reactions were run with: ddH_2O, 1X Ssofast™ EvaGreen® Supermix (Bio-Rad), 0.5uM Forward Primer, 0.5uM Reverse Primer, and 1µl mink cDNA sample. In brief, the reaction mix containing the water, Ssofast™ EvaGreen® Supermix (Bio-Rad), and specific primers was measured into an Eppendorf epMotion 5075 mastermix reservoir. Five microlitres of cDNA from each sample was loaded onto a 96-well PCR plate. Two additional wells were loaded with water alone to act as blanks, or 'no template controls'. A tube containing 90µl Tris Cl, pH 7.4 and 10µl of the working stock 0.01x standard was mixed as the starting point to prepare a 5-fold serial dilution series. The 96-well plate and standard tube were then transferred to the epMotion 5075 where the 384-well plate was prepared by the epMotion for the qRT-PCR run.

In brief, the epMotion protocol is as follows: the mastermix is mixed 7 times using an 8-well multichannel pipettor. The mastermix container is then removed and mixed manually by rocking side to side three times to ensure thorough mixing (to prevent the formation of a glycerol gradient from side to side, as sometimes occurs in very viscous mastermixes). The mastermix was then re-inserted into the machine. 45µl of mastermix was transferred from the reservoir into each sample-containing well of the 96-well plate and mixed two times. Ten microlitres of each mixed sample was then transferred to each of three well of the 384-well plate. Mastermix was then pipetted into the wells containing the blanks and then 10µl transferred to the 384-well plate as before. The standard curve dilution series was prepared by transferring 80µl of Tris Cl, pH 7.4 from a tube into each of 9 wells on a second empty 96-well plate. Sixty microlitres of the first dilution (already made, see above), was transferred to one well on the plate. Then

20µl was removed and mixed into the next well containing 80µl of Tris Cl, mixed, and 20µl removed to and transferred to the next well containing 80µl of Tris Cl, and so on until all 9 wells contained a dilution. The dilutions were then loaded, 5µl, onto the 96-well sample plate, mixed with 45µL of mastermix, and then 10µl of each loaded onto the 384-well plate. The plate was then transferred to the Lightcycler®480. Each sample was tested in triplicate with an acceptable coefficient of variation <10%.

Run conditions were 1 cycle of 30 seconds at 95°C, followed by 35 cycles of denaturation at 95°C for 5 seconds, annealing and extension at 58°C for 20 seconds, followed by a 1 cycle melt curve.

4.4.7 Data Normalization

Data was normalized to correct for sample-to-sample variation including tissue mass or cell number, RNA quality or quantity, or experimental treatment effects (Wong and Medrano, 2005). Two housekeeping genes (HKG) were tested. A housekeeping gene is an internal standard that is used to normalize the target results. A good housekeeping gene is expressed in all cells of the tissue where the target is located, has the same copy number in all cells, and resists changes in copy number in response to experimental conditions. The housekeeping gene, 18S ribosomal RNA, was used because it has been shown previously to resist change in expression in carnivores regardless of experimental conditions (Nieminen et al. 2010). The mastermix consisted of: ddH_2O, 1X PCR Buffer, 4.5mM $MgCl_2$, 0.2mM dNTP mix, 0.3mM of each primer, 0.8U Taq DNA Polymerase (Invitrogen), 0.25X SYBR Green I. The forward and reverse primers used for 18S rRNA are listed in Table 3. Reaction conditions on the LightCycler®480 were: 1 cycle at 95ºC for 5 minutes, 32 cycles consisting of 10 seconds at 95ºC, 20 seconds at

61ºC, and 30 seconds at 72ºC, and a melt curve of 1 cycle from 70ºC-95ºC and holding at 95ºC.

The second housekeeping gene tested was glyceraldehyde-3-phosphate dehydrogenase (GAPDH), as it was recently identified as a good normalizing gene for liver molecular research (Svobodova et al. 2008; Li et al. 2011). Glyceraldehyde-3-phosphate dehydrogenase was also run using the 384-well plate. The plate was prepared by the robot in the same manner as above. The mastermix consisted of: 1x GoTaq Flexi Buffer, 2.5mM $MgCl_2$, 0.2mM dNTP mix, 0.4µM each of GAPDH forward and reverse Primer, 0.8U GoTaq HS DNA Polymerase (Bio-Rad), and 1x EvaGreen® (Biotium). The forward and reverse primers used for GAPDH are listed in Table 3. Run conditions on the LightCycler®480 were: A hot start cycle of 1 cycle of 2 minutes at 95ºC, a PCR of 40 cycles at 95ºC for 10 seconds, 61ºC for 20 seconds, and 72ºC for 30 seconds, followed by a melt of 1 cycle.

Raw data from each normalizing gene (HKG) was analyzed using Proc Mixed in SAS® v.9.1 (SAS Institute Inc., Cary, NC, USA) to check that there was no effect of sex or group on concentration of rRNA. All GRP78 data was normalized by dividing the concentration of GRP78 by that of the HKG to produce the normalized dataset. This dataset was then statistically analyzed using the Proc Mixed program in SAS® v.9.1 (SAS Institute Inc., Cary, NC, USA). Results were reported as the ratio of number of copies of GRP78 to the number of copies of the HKG normalizing control so that results are shown as the gene of interest mRNA/HKG.

4.4.8 Controls

No reverse transcriptase (no RT) controls were run to check for DNA contamination of the RNA. Five mink liver RNA samples were chosen for testing. RNA from each sample was pipette into its own tube of a labeled 8-well strip. RNAse free ddH_2O was added to each tube. A 1/10 dilution using ddH_2O as the diluent was made of these controls into another 8-well strip. The no RT controls were run as a separate assay.

The housekeeping gene, GAPDH mRNA, was used as the normalizing factor and as confirmation that the RNA was of high quality resulting in good cDNA. Salt contamination control was achieved by assessing the ratio of the A260 / A230 readings when the concentration of the RNA was quantified by optical density at 260 nm using the Nanodrop ND1000 spectrophotometer (Thermo Fisher Scientific, Delaware, USA). A ratio greater than 1.8 indicated lack of salt contamination. The efficiency of each run had to be higher than 0.8 (80%), with R^2 values over 0.97 (97%). The samples were run in triplicate, and the maximum acceptable coefficient of variation (CV) for the triplicates was 10%. CV was calculated for each sample by dividing the standard deviation of the technical replicates by the mean Ct value of the same. Combined CV was calculated as the square root of the sum of the squares of the CV of GRP78 and GAPDH.

4.5 Statistical Analysis

The experimental design was a 2 x 6 factorial. There were two sexes and six treatment groups. All data obtained from this experiment was statistically analyzed using the Proc Mixed procedure in SAS® v.9.1 (SAS Institute Inc., Cary, NC, USA) to examine the effects of sex, and fasting regime and their interaction on liver NAI and to examine

the effects of sex and fasting regime and their interaction on liver GRP78 mRNA expression.

Both housekeeping genes were tested for sex and treatment effects. Additionally, since the 18S rRNA assay was run in three blocks using 96-well plates, a blocking factor was also tested for this gene. Glyceraldehyde-3-phosphate dehydrogenase was selected as the HKG for further analysis. GRP78 mRNA data were normalized using GAPDH mRNA before statistical analysis. Data were expressed as the ratio of GRP78/GAPDH. A P-value <0.05 was considered statistically significant.

Table 3. A, B, C, D: Primer pairs used to amplify mink specific GRP78 nucleotide sequence for sequencing. T7 Promotor primer pair for *in vitro* transcription to produce template copy RNA to be reverse transcribed to produce qPCR standards. E and F: Primers designed for mink GRP78 mRNA qRT-PCR assay; F: the final working primers.

Primers/ Gene rRNA	Forward Primer	Reverse Primer	Product Length	Genbank Accession Number
A (F15s R921s)	5'-CAGAGCTGTGCAGAAACTCC-3'	5'-CTCCCAGGCTTTCCTTTTTC-3'	907	XM_002916311 GD184947
B (F38s R928s)	5'-GGGAGGTAGAAAAGGCCAAA-3'	5'-AGTTTCCCTCCCAGGCTTT-3'	891	XM_002916311 GD184947
C (F255s R842s)	5'-TGGTGGCTCTACTCGAATCC-3'	5'-CGCTCCTTGAGCTTTTTGTC-3'	588	XM_002916311
D (F60s R493s)	5'-GGCCCTGTCTTCTCAACATC-3'	5'-CGGTGTTCCTTGGAATCAGT-3'	434	XM_002916311 GD184947
T7/dT promoter (F232 R659)	5'-TAATACGACTCACTATAGGGAGCATA TGGTGCTGCTGTCC-3'	5'-ttttttttttCTTCAGGTGTCAGGCGATTT -3'	458	HQ003898.1
E (F285 R371)	5'-CAGGTGATCTGGTACTGCTTG-3'	5'-TGTTCCTTGGAATCAGTTTGG-3'	90	HQ003898.1
F GRP78 Working Primers (F501 R611)	5'-TGACTGGAATTCCTCCTGCT-3'	5'-TGTTGCCTGTACCCTTGTCTT-3'	111	HQ003898.1
18S (F881 R1099)	5'-CGCGGTTCTATTTTGTTGGT-3'	5'-AGTCGGCATCGTTTATGGTC-3'	219	X01117
GAPDH (F36 R119)	5'-AATGCCTCCTGTACCACCAA-3'	5'-GGTCATGAGTCCCTCCACAA-3'	84	AF076283

Table 4. Mink specific nucleotide and amino acid sequences for glucose regulated protein 78 submitted to GenBank (NCBI).

	Accession #	Sequence
Mink GRP78 mRNA nucleotide sequence	HQ003898.1	CTTCTCTGAGACTCTGACACGGGCCAAATTTGAAGAGCTAAATATGGACCTGTTCCGTTCGA CCATGAAGCCTGTCCAGAAGGTGCTAGAGGATTCTGACTTAAAGAAGTCTGATATTGATGA AATTGTTCTTGTTGGTGGCTCTACTCGAATCCCAAAGATTCAACAACTGGTTAAAGAGTTCT TCAATGGCAAGGAGCCATCCCGTGGCATCAACCCAGATGAGGCTGTAGCATATGGTGCTGC TGTCCAGGCTGGTGTACTCTCTGGTGATCAAGATACAGGTGATCTGGTACTGCTTGATGTAT GTCCCCTTACACTTGGTATTGAAACTGTGGGAGGCGTCATGACCAAACTGATTCCAAGGAAC ACCGTGGTGCCCACCAAGAAGTCTCAGATCTTTTCTACAGCTTCTGATAACCAACCAACTGT TACAATCAAGGTCTATGAAGGTGAACGACCCCTTACAAAAGACAATCACCTTCTGGGAACT TTTGATCTGACTGGAATTCCTCCTGCTCCCCGTGGAGTCCCACAGATTGAAGTTACCTTTGA GATAGATGTGAATGGCATTCTTCGAGTGACAGCTGAAGACAAGGGTACAGGCAACAAAAAC AAGATTACAATTACCAATGACCAAAATCGCCTGACACCTGAAGAAA
Protein amino acid sequence	ADM18967.1	FSETLTRAKFEELNMDLFRSTMKPVQKVLEDSDLKKSDIDEIVLVGGSTRIPKIQQLVKEFFNGKE PSRGINPDEAVAYGAAVQAGVLSGDQDTGDLVLLDVCPLTLGIETVGGVMTKLIPRNTVVPTKK SQIFSTASDNQPTVTIKVYEGERPLTKDNHLLGTFDLTGIPPAPRGVPQIEVTFEIDVNGILRVTAE DKGTGNKNKITITNDQNRLTPEE

Table 5. Comparison of mink specific GRP78 mRNA nucleotide sequence (Accession # HQ003898.1) to other species.

Species	Accession Number	% Identity
Human HspA5	NM_005347.4	94%
Dog GRP78	XM_858246.1 / XM_537847.2	97% / 96%
Panda GRP78	XM_002916311.1	97%

Table 6. Comparison of mink specific GRP78 protein amino acid sequence (Accession # ADM18967.1) to other species.

Species	Accession Number	% Identity
Human HspA5	NP_005338.1	100%
Dog GRP78	XP_863339.1 / XP_537847.2	100% / 95%
Panda GRP78	XP_002916357.1	100%

CHAPTER 5.0: RESULTS

5.1 Histology

Mallory-Denk bodies are identified by the characteristic hyaline deposits in the hepatocyte cytoplasm. In Masson's Trichrome stained liver sections fibrosis was identified by blue staining of collagen fibers. Neither Mallory-Denk bodies nor fibrosis were observed in the Masson's Trichrome prepared liver sections.

Analysis of liver NAI (grade) showed both a sex and group effect but no interaction effect (Table 7). Overall, males showed higher NAI than females (4.81±0.262 for males, 3.64±0.259 for females; Table 8, Figure 9) indicating a larger volume of stored lipid in the liver overall. All groups showed mild fat accumulation (NAI = 1.90±0.445, 2.90±0.445, 3.50±0.445, 2.95±0.472 for 0day, 1day, 3day, and RF respectively; Table 7, Figure 8) based on the NAI method of grading lipid accumulation used in humans (Merat et al. 2010) except for the 5day and 7day group, which showed moderate lipid accumulation (NAI=7.33±0.472 and 6.77±0.426 for day 5 and day 7 respectively).

The liver NAI results were supported by the liver histology micrograph figures which follow, showing that fat accumulation in the liver tissue increased as length of fasting was increased. The day 0, 1, and 3 groups showed largely normal liver architecture (Figures 2, 3, and 4); organized plates of hepatocytes radiating from the central vein to the cell periphery, organized un-distended sinusoids, low number, or no, inflammatory cells present. The day 5 and 7 livers (Figures 5, and 6) showed greater deposition of lipid in the hepatocytes, pushing the cell nuclei to the periphery. Cells containing the largest amount of lipid were located around the portal triads. Hepatocytes were disorganized and sinusoids appeared swollen and also disorganized. Inflammatory

cells were present in the portal areas. Livers of the mink in the re-fed group appeared to have recovered the liver architecture of the pre-fasted animals (Figure 7).

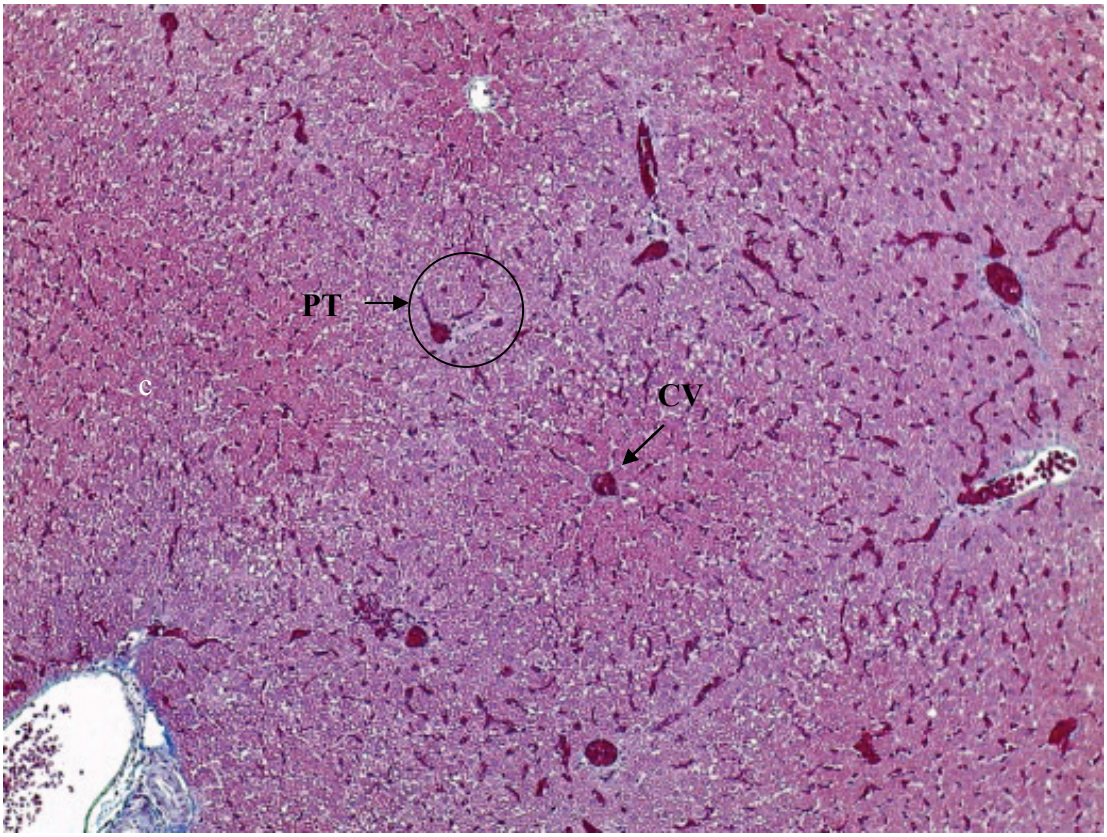

Figure 2. Liver morphology in control mink. Liver morphology appears normal. Plates of hepatocytes are orderly and radiating outward from the central vein to the lobule periphery. CV: Central Vein, PT: Portal Triad. Magnification 100x.

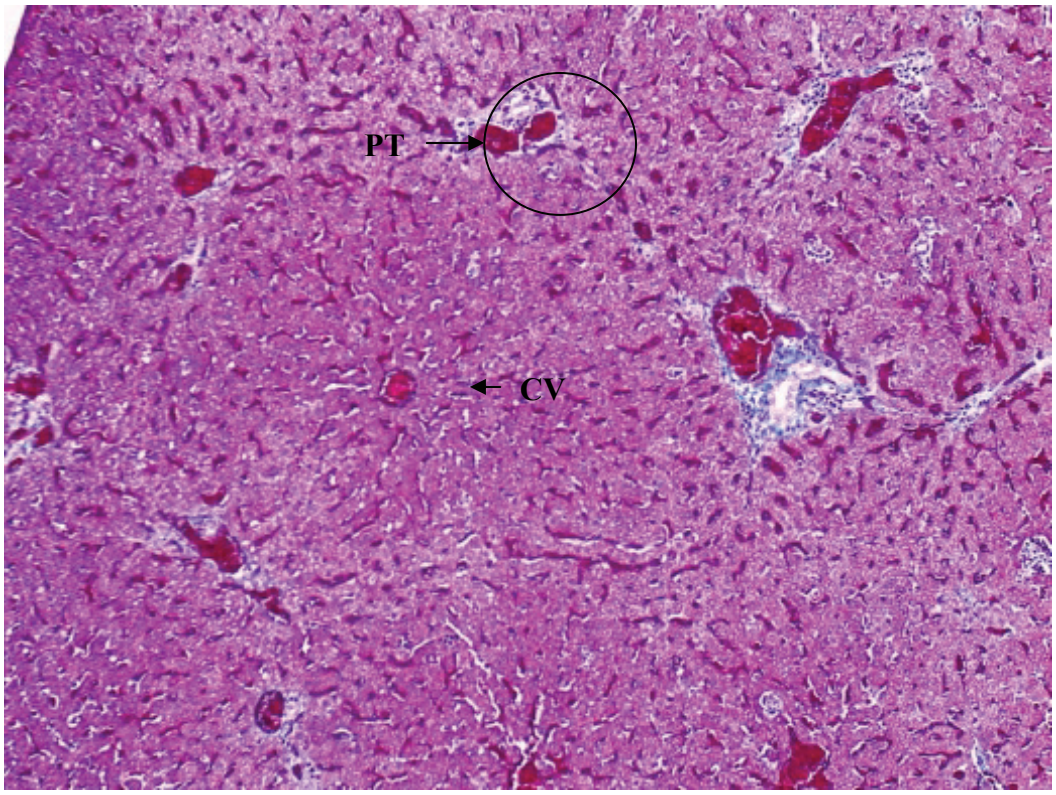

Figure 3. Liver morphology in mink fasted for 1 day. Liver morphology appears normal. Plates of hepatocytes are orderly and radiating outward from the central vein to the lobule periphery. CV: Central Vein, PT: Portal Triad. Magnification 100x.

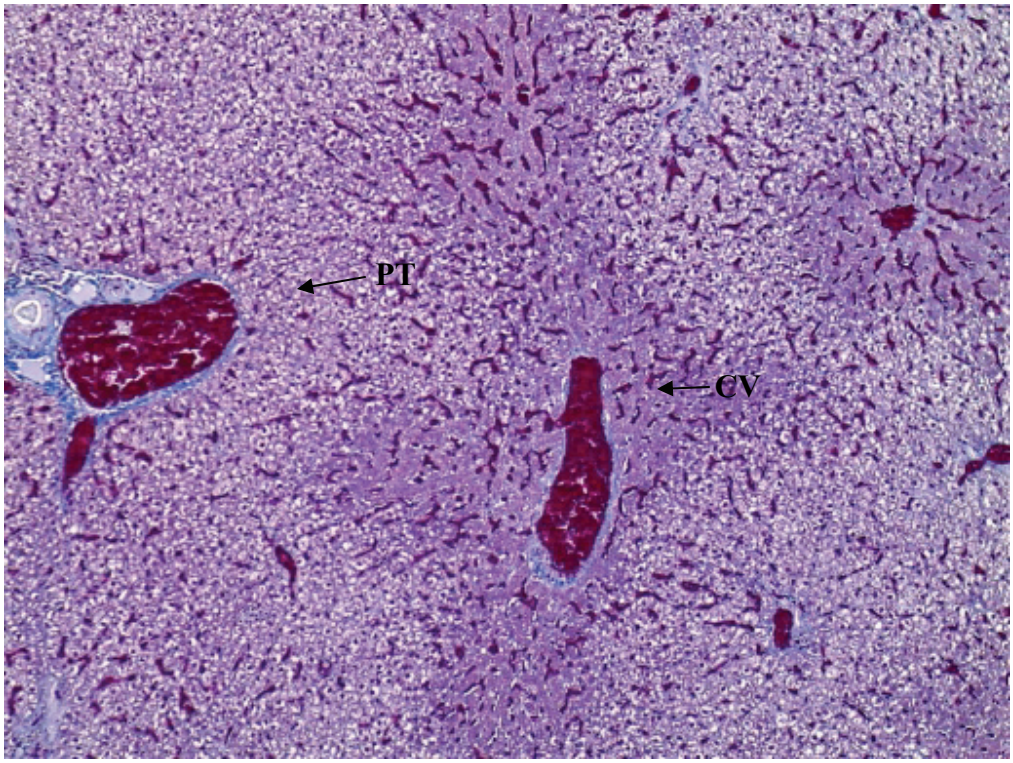

Figure 4. Liver morphology in mink fasted for 3 days. Liver morphology is still largely normal. However, some hepatocyte lipid accumulation is evident peri-portally. CV: Central Vein, PT: Portal Triad. Magnification 100x.

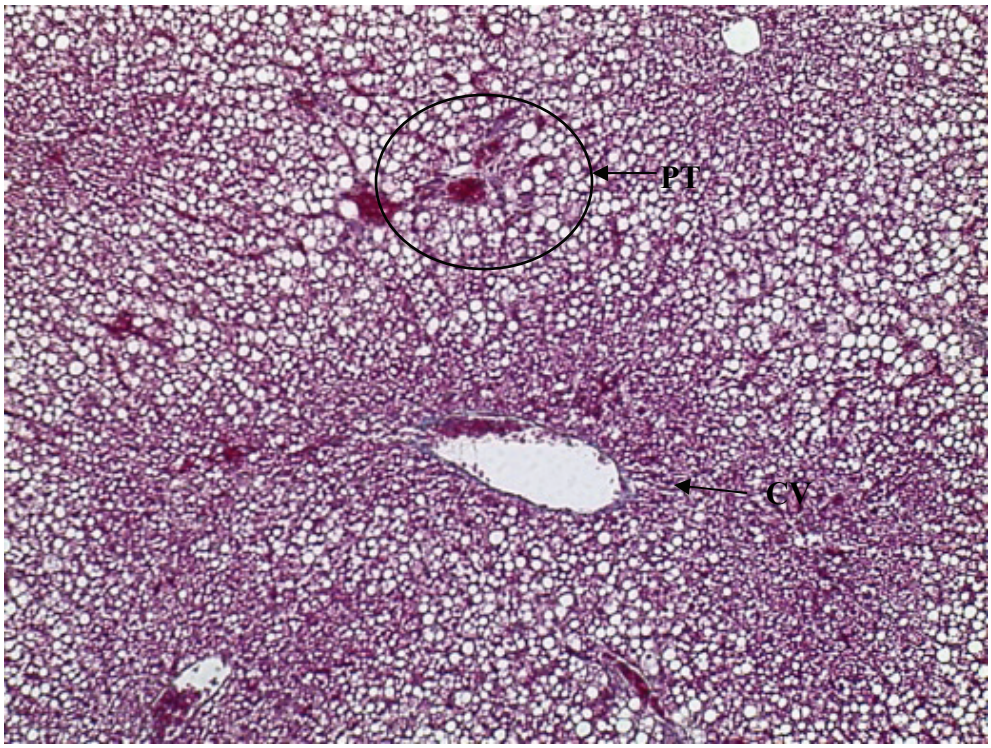

Figure 5. Liver morphology in mink fasted for 5 days. Lipid accumulation in hepatocytes is evident. Lipid accumulation is pushing the nuclei to the hepatocyte cell periphery. Hepatocytes are disorganized and sinusoids are compressed. Hepatocyte lipid accumulation is most severe peri-portally. CV: Central Vein, PT: Portal Triad. Magnification 100x.

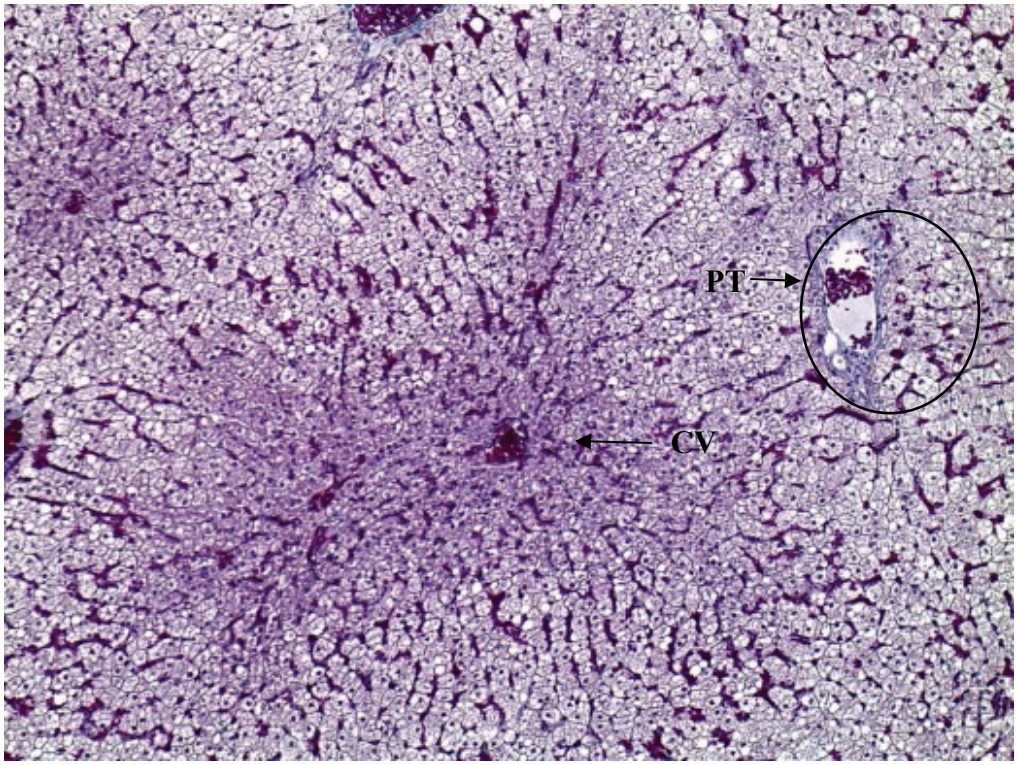

Figure 6. Liver morphology in mink fasted for 7 days. Moderate lipid accumulation in hepatocytes is evident; hepatocyte lipid accumulation is most severe peri-portally. Lipid accumulation is pushing the nuclei to the hepatocyte cell periphery. Hepatocytes are disorganized and sinusoids are compressed. CV: Central Vein, PT: Portal Triad. Magnification 100x.

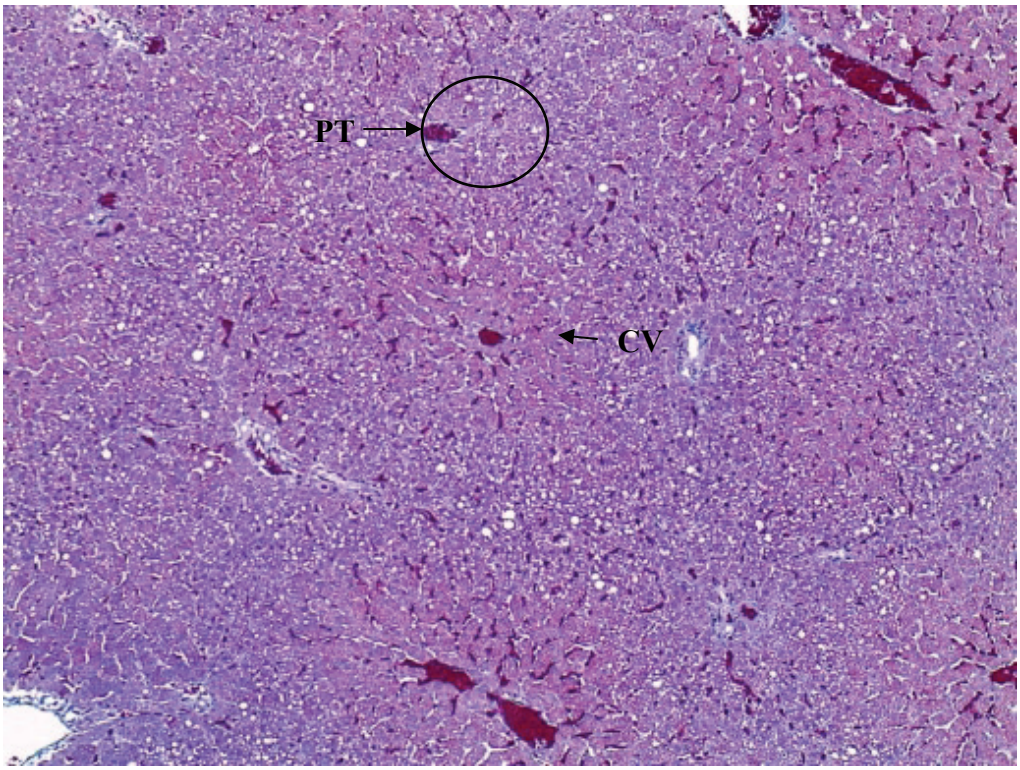

Figure 7. Liver morphology in mink re-fed for 28 days. Liver morphology returned to the pre-fasted state. Plates of hepatocytes are orderly and radiating outward from the central vein to the lobule periphery. CV: Central Vein, PT: Portal Triad. Magnification 100x.

5.2 Glucose Regulated Protein 78 Messenger Ribonucleic Acid Levels

The 18S rRNA and GAPDH mRNA normalizing genes were evaluated in SAS to ensure no significant effect of sex or experimental treatment on concentration. The 18S rRNA showed a block effect and a marginal sex effect on concentration but the GAPDH showed no significant effect by sex or treatment on concentration (Table 9). Blocking effect was not applicable for GAPDH as all samples were run at once using a 384-well plate. Therefore, the GRP78 data was normalized using the GAPDH mRNA data.

Analysis of normalized GRP78 mRNA levels showed a sex and group effect but no sex × group interaction (Table 10). Overall, females showed greater expression of GRP78 mRNA than males (Table 11, Figure 11). With respect to group, mink fasted for 7 days showed significantly higher expression of GRP78 mRNA than any other group (Table 12, Figure 10). Mink fasted for 0, 1, 3, or 5 days showed significantly lower GRP78 mRNA levels from the 7 day group but were not statistically different from one another. The re-fed group showed no difference in GRP78 mRNA expression from the 0 day control group but was significantly lower than any of the other groups.

The GAPDH mRNA coefficient of variation (CV) was 1.2%. The GRP78 assay CV was 3.9%. The combined assay CV was 0.04%.

Table 7. P-values for effect of sex, fasting, and sex × fasting on liver NAI mink. LSmeans ±SE shown for the effect of fasting on liver NAI in mink. Letter groupings indicate significant differences for fasting effect. LSmeans of 0 = no fatty liver, 1-4 = mild fatty liver, 5-8 = moderate, 9-12 = severe. Differing letters indicate significant differences between groups (P<0.05).

Variable	Group						P-value		
	Day 0	Day 1	Day 3	Day 5	Day 7	RF	Sex	Fasting	Sex × Fasting
NAI	1.90±0.445c	2.90±0.445bc	3.50±0.445b	7.33±0.472a	6.77±0.426a	2.95±0.472bc	**<0.001**	**0.003**	0.889

Table 8. Effect of sex on NAI expressed as LSmeans ±SE. Overall, males always showed higher NAI scores than females. P<0.05 indicates statistical significance.

Variable	Sex		P-value
	Male	Female	
NAI	4.81±0.262	3.64±0.259	**0.003**

Table 9. P-values of the main effects and interaction for the normalizing genes 18S rRNA and GAPDH mRNA. P<0.05 indicates statistical significance. Bolded numbers indicate significance or a trend (P<0.01).

Effect	18S rRNA	GAPDH mRNA
	P-value	
Block	**0.013**	N/A
Group	**0.067**	0.125
Sex	0.701	0.443
Group*Sex	0.147	0.345

Table 10. P-values for analysis of GRP78/GAPDH ratio in mink fasted 0, 1, 3, 5, or 7 days or fasted for 7 days followed by a period of re-feeding of 28 days. P<0.05 indicates statistical significance.

Effect	P-value
Group	**<0.001**
Sex	**0.050**
Group*Sex	0.160

Table 11. Effect of sex on GRP78/GAPDH ratio, expressed as LSmeans ±SE. Differing letters indicate significant difference between sexes (P<0.05).

Variable	Sex		P-value
	Male	Female	
GRP78	0.311±0.024 b	0.379±0.024 a	**0.050**

Table 12. Multiple means comparison for the effect of length of fast (group) on GRP78/GAPDH ratio in mink expressed as LSmeans ±SE. LSmeans of 0 = no fatty liver, 1-4 = mild fatty liver, 5-8 = moderate, 9-12 = severe. Differing letters indicate significant differences between groups (P<0.05).

Variable	Group					
	Day 0	Day 1	Day 3	Day 5	Day 7	RF
GRP78	0.267±0.041bc	0.342 ±0.041b	0.319±0.041b	0.371±0.041b	0.569±0.039a	0.201±0.043c

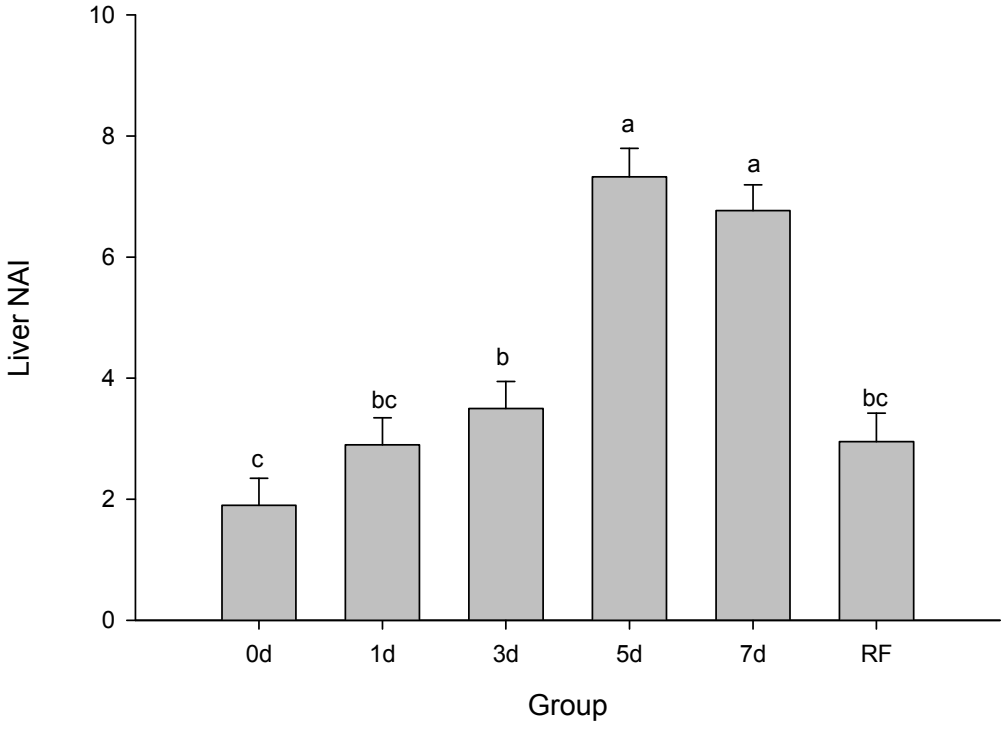

Figure 8. Effect of fasting on liver NAI in mink fasted 0, 1, 3, 5, or 7 days or fasted for 7 days followed by a period of re-feeding of 28 days. Differing letters indicate significant differences between groups ($P<0.05$).

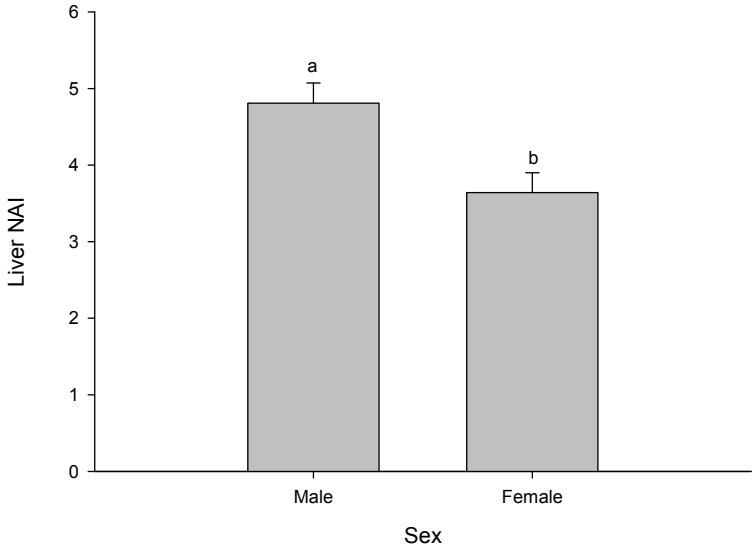

Figure 9. Effect of fasting on liver NAI in male and female mink, all groups combined (n=30 per sex). Differing letters indicate significant difference between sexes ($P<0.05$).

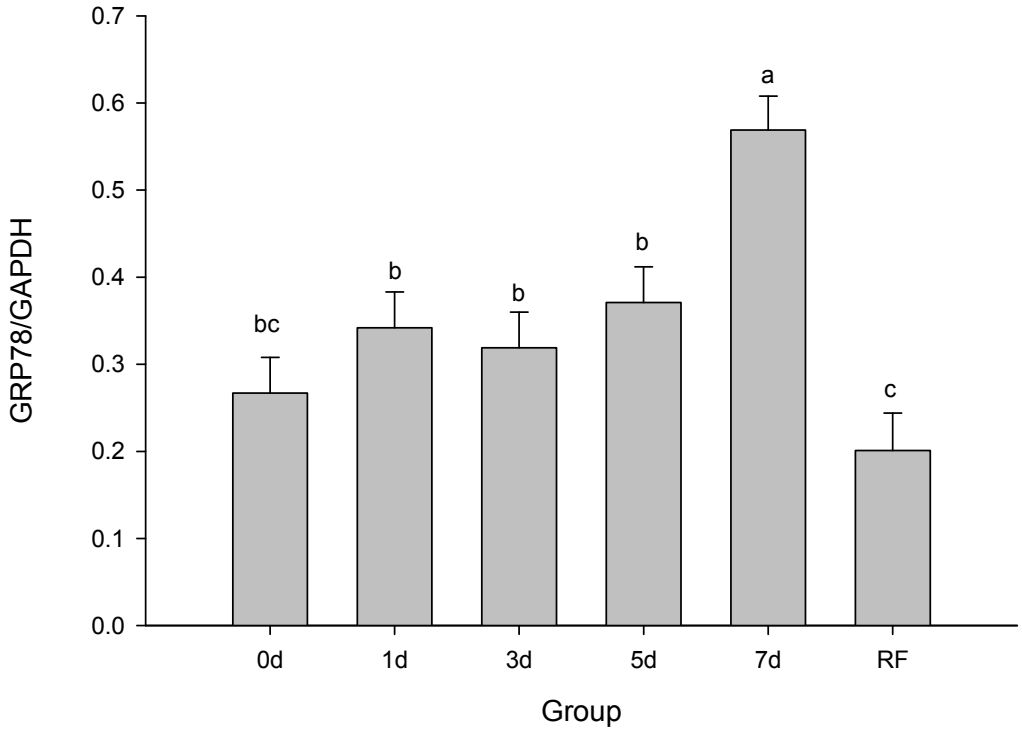

Figure 10. Effect of fasting on liver GRP78/GAPDH ratio in mink fasted 0, 1, 3, 5, or 7 days or fasted for 7 days followed by a period of re-feeding of 28 days. Differing letters indicate significant differences between groups ($P<0.05$).

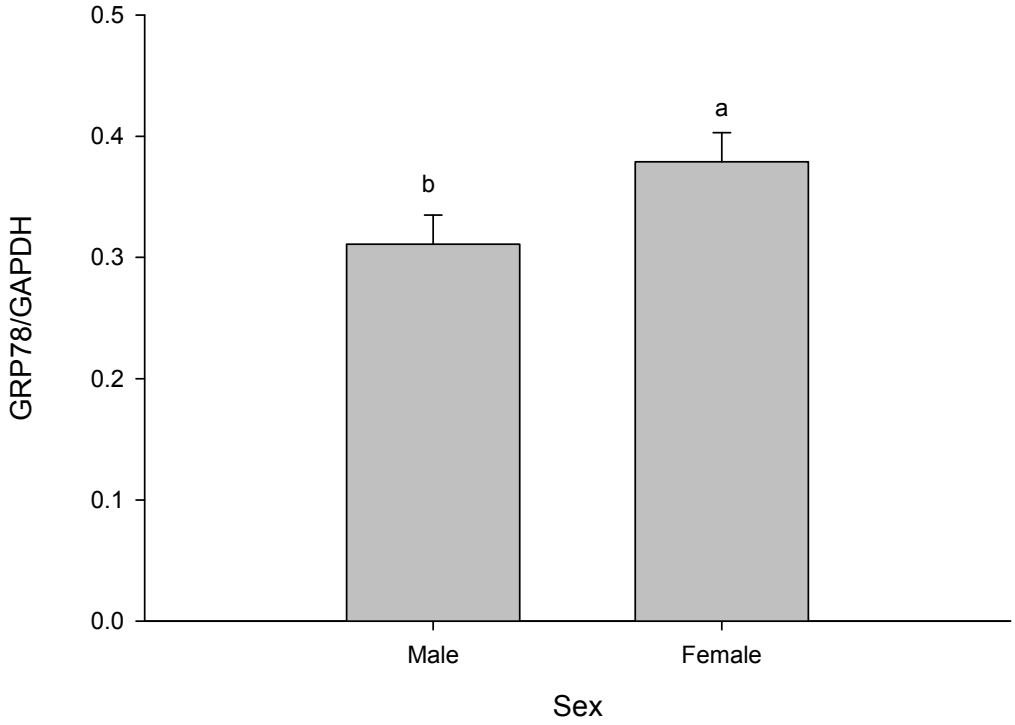

Figure 11. Effect of fasting on liver GRP78/GAPDH ratio in male and female mink (n=30 per sex). Differing letters indicate significant difference between sexes ($P<0.05$).

CHAPTER 6.0: DISCUSSION

6.1 Development of Simple Fatty Liver and Progression to Steatohepatitis

In addition to humans, fasting has been shown to induce simple steatosis in mink and other carnivores (Bjornvad et al. 2004; Mustonen et al. 2005a; Mustonen et al. 2006; Nieminen et al. 2009). The histological evaluation method outlined by Merat et al. (2010), used in humans, was applied to characterize the progression of simple fatty liver to steatohepatitis in the mink. The images in Figures 2-7 are representative of the fat content seen in each group over the course of the fasting experiment.

There was no significant difference seen between the 0 day, 1 day, and re-fed groups with regards to NAI score and no difference between the 1 day, 3 day, and the re-fed group (Table 7, Figure 8). All of these groups had mean NAI values between 1 and 4 which puts them into the mild category of fatty liver disease (Merat et al. 2010). There was no significant difference between the 5 and 7 day fasted groups (Table 7, Figure 8). Both of these groups had mean NAI values between 5 and 8 which place them in the moderate category of fatty liver disease according to Merat et al. (2010). Supportively, significantly increased liver lipid % was found in these same mink by the third day of fasting (Rouvinen-Watt et al. 2010). The reported liver lipid percentages for the 0, 1, 3, 5, 7-day, and RF groups were 5.9 ± 1.5, 6.1 ± 1.5, 13.2 ± 1.5, 19.0 ± 1.5, 19.7 ± 1.4, and 5.3 ± 1.6, respectively (Rouvinen-Watt et al. 2010).

The NAI results suggest that fasting causes progression of fatty liver in mink from mild to moderate by the fifth day of fasting. However, it is difficult to state this with certainty because the control mink were not true controls. According to the liver NAI results (Table 7) and classification scheme of Merat et al. (2010) the control mink (day 0)

had mild fatty liver (1.90±0.445) at the onset of this experiment. This is in agreement with results reported by Rouvinen-Watt et al. (2010) that these mink had a liver fat content of 5.9% and body fat percent of 33% at the onset of fasting, indicating that these mink could be considered obese. The current findings are supported by Dick (2010) who investigated the effects of body condition on the development of fatty liver in mink. She found that obese mink, fed at 120% of their recommended dietary allowance, when subjected to a 5-day fast, deposited significantly greater amounts of lipid in the liver than lean mink, which were fed at 80% of their recommended dietary allowance prior to fasting. Obesity is a well known risk factor which increases the likelihood of fatty liver disease development in humans (Marceau et al. 1999; Toshimitsu et al. 2007) and this appears to be the case also in the mink.

Another consideration is the natural weight fluctuations seen in mink annually. Previous reports have shown that mink tend to lay down greater amounts of fat in the body in the autumn months, likely as an adaptive response to possible food scarcity in the winter months (Rouvinen and Kiiskinen 1989). This, coupled with *ad libitum* feeding practices may have been responsible for the over-conditioning of the mink at the onset of this experiment.

Since these mink had mild fatty liver at the onset of this trial, according to the evaluation scheme used (Merat et al. 2010), it may be suggested that mink in most commercial production systems likely are as well, if the producers are following the same *ad libitum* feeding regime. These mink are at a greater risk of developing fatty liver disease, and the associated co-morbidities, described in mink and other carnivores during high stress periods in the production cycle (Rouvinen and Kiiskinen 1989; Korhonen and

Niemelä 1997; Tauson 1984; Hunter and Schneider 1996). Overweight mink will be at greater risk of developing fatty liver in response to rapid flushing in preparation for breeding, and during the high stress periods of parturition and mid-lactation when energy demands are the greatest (Rouvinen and Kiiskinen 1989; Korhonen and Niemelä 1997; Tauson 1984; Hunter and Schneider 1996). It would benefit producers to establish feeding practices that promote maintenance of ideal body condition of the animals year round, especially at the time when females are selected for breeding, to reduce exposure of their animals to risk factors associated with fatty liver disease development. In addition to avoiding triggering fatty liver disease development, reducing the amount of feed given to the animals is also an economic benefit to producers.

Liver recovery to the pre-fasted levels is shown by the RF group (Table 7, Figure 8). These mink did not recover their initial body weight (1990.4 ± 78.6 final weight for the control group vs. 1650.9 ± 83.4 final weight for the RF group) but did show a return to pre-fasted liver lipid percentages (5.9 ± 1.5%, 6.1 ± 1.5 vs. 5.3 ± 1.6% for the control and RF groups, respectively; Rouvinen-Watt et al. 2010) along with return to baseline liver morphology (Table 7; Figure 8). A recent report by Pal et al. (2008), using histological assessment of hematoxylin and eosin stained liver sections from the same animal experiment, agrees with the Rouvinen-Watt et al. (2010) findings and this study showing that return to normal liver architecture from fasting induced simple fat accumulation in the liver is possible in mink after a period of re-feeding of four weeks post 7 day fast. That study used the Brunt et al. (1999) method to evaluate fatty liver disease presence and severity. It was found that by the third day of fasting significant

lipid accumulation had occurred over the control group. The re-fed group showed a return to normal pre-fasted liver architecture.

The liver fat increases in conjunction with the body weight loss were shown to originate largely from the intra-abdominal depots (Rouvinen-Watt et al. 2010). These findings agree with those reported in European pole cats, *Mustela putorius,* (Mustonen et al. 2009), sables, *Martes zibellina,* (Mustonen et al. 2006), and other studies on the effects of fasting in mink, *Neovison vison* (Bjornvad et al. 2004; Mustonen et al. 2005a). When mobilized, non-esterified fatty acids from the intra-abdominal adipose tissue are released directly into the portal circulation (Smith and Schenk 2000), large amounts of non-esterified fatty acids are delivered to the liver to be used for energy and a large proportion end up in storage, increasing the liver fat percent. The liver normally stores small amounts of lipid but is not a major storage organ. Normally, lipids delivered to, or produced by, the liver are exported by very low density lipoprotein, or metabolized via beta-oxidation by the mitochondria (Videla et al. 2004). Accumulation and storage occur when the delivery of non-esterified fatty acids and production of lipid by the liver exceed its ability to metabolize or secrete it.

The return to pre-fasted NAI levels in this study along with the liver fat percent and body weight data reported by Rouvinen-Watt et al. (2010) for the same mink suggests that a return to baseline health is possible in the mink even after 7 days of food deprivation. Benign simple fatty liver has been shown to be reversible in humans (Mantena et al. 2008; Tannapfel et al. 2011). Based on these results it is evident that mink food deprived for up to 7 days do not show progression to the more severe and life threatening condition, steatohepatitis.

The report by Rouvinen-Watt et al. (2010) found that the females used in this study lost a greater percentage of body weight over the fasting period than the males. It could be expected that this would correlate with mobilization of a greater amount of fat to the liver via the portal circulation. However, the liver NAI results suggest the opposite. Overall, the liver sections of the male mink contained more lipid droplets than the liver sections of the female mink (Table 8, Figure 9). This may be due to the sexual dimorphism of the species, as the males are nearly twice as large as the females (Korhonen and Niemelä 1997; Thom et al. 2004). Give the pronounced difference in the metabolic body size, the females would be more energetically challenged during cold weather, which could have further increased fat oxidation to meet energy demands. Therefore, it is likely that the female mink may have experienced greater hepatic fatty acid oxidation, which may have reduced the liver lipid deposition in the females in comparison to the males during rapid body fat mobilization.

The NAI method is modified from the Brunt (1999) and the Kleiner et al. (2005) methods and may still require some adjustment because it is a subjective measurement. Evaluator experience and training play a large role in the outcome. Perhaps using computer software to analyze the slides (i.e. to identify presence of marking criteria and to judge severity) would remove much of the subjectivity and yield different results. Additionally, this method has been designed for use in evaluating human sample and may not be optimal for use in mink. The day 0 non-fasted mink in this study have mild fatty liver according to the Merat et al. (2010) method. While this may be accurate, as these mink had a liver fat of nearly 6% and could have been considered obese at the onset of this trial (Rouvinen-Watt et al. 2010), perhaps this is an indication that the method needs

to be adjusted to account for differences in mink and human normal liver lipid content. In the diagnosis of fatty liver in humans a 5% liver lipid content is used as the threshold for the development of NAFLD (Brunt et al. 1999). In mink, previous research has shown that normal liver lipid content may vary from 2 to 9.4% (Kannan et al. 2002; Clausen and Sandbøl 2004; Mitchell and Rouvinen-Watt 2008). Still others have suggested a threshold between 9 and 12% (Käkelä et al. 2001; Rouvinen-Watt et al. 2010). Performing a study using lean, normal, and obese mink phenotypes to test the Merat et al. (2010) NAI method would assist in determining the suitability of this method for further mink histological grading of mink liver sections.

Mink do appear to naturally deposit greater amounts of adipose tissue in the intra-abdominal depots, in comparison with other adipose depots, when obese (Rouvinen-Watt et al. 2010). In humans, large amounts of intra-abdominal fat are thought to pre-dispose to fatty liver disease development and be a risk factor for progression to steatohepatitis (Westphal 2008). Obesity has also been identified as a risk factor of fatty liver disease development in cats (Dimiski and Taboada 1995; Wasserback York et al. 2009) and has been linked to the presence of fatty liver in mink (Hunter and Barker 1996). Mink may be at a greater risk of developing fatty liver disease due to the natural preference for intra-abdominal fat storage during the lipid storage process and preferential mobilization from this area during fasting. For this reason, it may be more beneficial to producers to maintain both male and female mink at a constant ideal body condition rather than encouraging excessive feed consumption in order to produce larger pelts or rapidly slimming down females in preparation for breeding.

6.2 Presence of Mallory-Denk Bodies, and Fibrosis

According to the Merat et al. (2010) method of steatohepatitis identification, through the pairing of the NAI and the staging procedures, it is evident that while fatty liver did develop in the mink in the current study, progression to steatohepatitis did not occur. There was no indication of either Mallory-Denk body formation or fibrosis in the Masson's Trichrome stained liver sections. Since MDBs are the morphologic hallmark of steatohepatitis in humans (Brunt 2005) and the presence of fibrosis is indicative of progression to steatohepatitis from simple fatty liver disease (Merat et al. 2010), it can be suggested that these mink fasted for a period of 7 days did not develop steatohepatitis. Therefore, the mink in this study likely experienced the first hit, simple steatosis/benign lipidosis, in the two hit hypothesis for fatty liver disease (Day 2002). Though this may not be a severe enough condition to cause serious illness, as the mink in the study were asymptomatic and appeared healthy (Rouvinen-Watt et al. 2010), the livers may have been predisposed to the second hit of oxidative stress (Malínská et al. 2010), an indication of which is the presence of up-regulated GRP78 mRNA.

6.3 Liver Glucose Regulated Protein 78 and Endoplasmic Reticulum Stress

Production of reactive oxygen species and development of oxidative stress have been reported in conjunction with the development of steatohepatitis, the second hit of NAFLD, in non-alcoholic steatohepatitis in humans (Day 2002; Videla et al. 2004). The molecular chaperone glucose regulated protein 78 (GRP78) is up-regulated in the livers of individuals who are suffering from oxidative stress and endoplasmic reticulum stress (Lee 2005). The mink in this study showed both group and sex effects on liver GRP78 mRNA levels but no interaction effects (Table 10). Since GRP78 up-regulation is

considered a marker of the development of endoplasmic reticulum stress, leading to oxidative stress and initiation of the unfolded protein response it may be suggested, based on these results, that this does occur within a fasting period of 7 days in the American mink. Significantly elevated GRP78 mRNA concentrations were found by 7 days of fasting in the mink (Table 12, Figure 10), while all other groups were not different from the baseline control group.

Increased phospholipid and phosphatidyl choline synthesis has also been reported in these same mink (Rouvinen-Watt et al. 2010). Studies have suggested that increased synthesis of these also indicates the presence of endoplasmic reticulum stress and induction of the unfolded protein response (Sriburi et al. 2004) which may lead to increased protein mis-folding in the ER, formation of Mallory-Denk bodies, induction of the inflammatory response, and progression of simply fatty liver to steatohepatitis (Hanada et al. 2007; Özcan et al. 2004).

In humans, fat accumulation in the liver as fatty liver disease progresses appears to pre-dispose the individual to increased plasma free fatty acids, an imbalance in the omega-3/omega-6 polyunsaturated fatty acid ratio, and development of insulin resistance (Marceau et al. 1999). These conditions have been suggested to predispose the liver to development of NASH (Balaban et al. 2006; Malínská et al. 2010) and have been reported in fasted mink and other carnivores (Nieminen et al. 2006; Mustonen et al. 2006; Rouvinen-Watt et al. 2010). Imbalances in liver fatty acids in conjunction with increased fat accumulation in the liver have been suggested as risk factors for the progression from simple NAFLD to NASH in humans (Malínská et al. 2010). An imbalance in omega-3/omega-6 PUFAs has been shown to favor the initiation of the inflammatory response in

the body. A previous study using these same mink found an imbalance in the omega-3/omega-6 PUFAs in conjunction with increased fat accumulation in the liver (Rouvinen-Watt et al. 2010).

Obesity is also associated with the pathogenesis of type-2 diabetes in humans and insulin resistance has been linked to hepatocyte lipid accumulation in people diagnosed with NAFLD (Aller et al. 2008). It has been proposed that obesity plays a role in ER stress and the development of insulin resistance in hepatocytes (Özcan et al. 2004). Disruption of glucose homeostasis has been reported in mink dams suffering from nursing sickness, of which fatty liver is often diagnosed post mortem (Wamberg et al. 1992; Clausen et al. 1992; Hynes and Rouvinen-Watt 2007ab). Prolonged insulin resistance leads to glucose/energy starving of the tissues and organs affected (Leclercq et al. 2007) and if not alleviated causes those cells to undergo apoptosis. Organs that are not protected by glucose channels, such as the brain, are continuously bathed in hyperglycemic blood. This can cause permanent damage to those organs (Pulsinelli et al. 1982). Overweight mink have also been shown to develop hyperinsulinemia (Rouvinen-Watt et al. 2004). The 0 day mink in this study had higher circulating levels of plasma insulin than the mink that were fasted or when the 7-d fast was followed by re-feeding (Rouvinen-Watt et al. 2010). Obesity could likely predispose the mink to the development of insulin resistance associated with fatty liver disease. Overweight and obese breeder females may therefore be at a greater risk of developing nursing sickness as suggested by Rouvinen-Watt (2003) or reproductive failure associated with early disruption in glucose homeostasis (Hynes and Rouvinen-Watt 2007a).

GRP78 levels have been shown to be elevated in obese people with insulin resistance triggered by increased fat accumulation in liver hepatocytes leading to ER stress (Özcan et al. 2004). The GRP78 mRNA results, taken together with the increased liver NAI, the elevated liver phospholipid and phosphatidylcholine levels, and the low plasma insulin concentrations (Rouvinen-Watt et al. 2010), but lack of MDB or fibrosis presence may suggest that perhaps these mink were on the cusp of developing steatohepatitis. Should they have been fasted longer it is likely they would have developed it along with the other markers of NASH. However, in humans development of NASH occurs over a long period of time (Powell et al. 1990) and this may also be the case for the mink.

Liver GRP78 mRNA results indicated that females overall show greater expression of GRP78 mRNA than did males (Table 13, Figure 11). Taken with the liver NAI results, where males showed greater accumulation of fat in the liver in general, this could suggest that females are metabolizing greater amounts of lipid due to their lower metabolic body size. This may lead to greater oxidative stress and ER stress as indicated by the greater elevation of the GRP78 mRNA levels. Additionally, results reported by Rouvinen-Watt et al. (2010) found decreased omega-3 polyunsaturated fatty acids in relation to omega-6 in the female mink livers over the males. This ratio favors induction of the inflammatory response and could lead to the progression of simple fatty liver to steatohepatitis (El-Badry et al. 2007). Therefore, female mink may be more prone to the development of oxidative stress during rapid body fat mobilization than the males.

An additional possibility for the up-regulation of GRP78, besides oxidative stress, could be glucose or nutrient deprivation, caused by fasting, leading to increased

gluconeogenesis and glucose depletion of the liver cells causing ER stress and up-regulating GRP78 in the liver (Özcan et al. 2004). It is possible that the female mink, due to their faster rate of metabolism, may be exhibiting increased gluconeogenesis and export of glucose from liver cells; a response characteristic of ER-stress initiated insulin resistance (Özcan et al. 2004). Further studies are needed to determine roles that oxidative stress, caused by lipid accumulation and metabolism, and hepatic glucose deficit may play in the development of ER-stress induced insulin resistance.

Analysis of the normalizing gene, 18S rRNA, revealed a trend toward significance in response to fasting treatment ($P = 0.067$, Table 9). This may have reduced the sensitivity of the statistical analysis of the GRP78 mRNA results. 18S rRNA has been the standard normalizing gene used in fatty liver research by the Carnivore Nutrition and Physiology research laboratory at the Nova Scotia Agricultural College, Truro, Nova Scotia, Canada, however, recent studies have shown that other housekeeping genes may be more suitable. Glyceraldehyde-3-phosphate dehydrogenase (GAPDH) has recently been suggested as a good normalizing gene for liver molecular research (Svobodova et al. 2008; Li et al. 2011) and proved to be a good normalizing gene for fatty liver research in mink in this study. No effect of sex or fasting regime on GAPDH mRNA concentration was seen in this assay (Table 9). GAPDH may also be a good normalizing control for research in other mustelids.

CHAPTER 7.0: CONCLUSION

Mink fasted for a period of 7 days show development of simple fatty liver by the fifth day of fasting. In contradiction to the hyptothesis, they do not show Mallory-Denk body formation or fibrosis in histologically prepared liver sections. As Mallory-Denk body formation is regarded as the morphologic hallmark of steatohepatitis, and fibrosis is considered a key characteristic of livers afflicted by steatohepatitis it can be considered that these mink did not develop steatohepatitis over the course of this experiment. However, liver mRNA levels of the molecular chaperone used as a marker of endoplasmic reticulum stress, GRP78, were increased in response to the 7-day fasting regime which agrees with the hypothesis. This suggests that mink may be developing endoplasmic reticulum stress, leading to oxidative stress and initiation of the unfolded protein response by 7 days of food deprivation. This may be indicative of entrance into the earliest stages of steatohepatitis development however further study is needed to confirm this.

Recovery of liver morphology and GRP78 mRNA expression to pre-fasted levels was found in the mink in this study, agreeing with previous reports and the hypothesis of this study, that return to original control condition from simple fatty liver disease is possible.

REFERENCES

Abdel-Malek M, Diehl A. Mechanisms underlying non alcoholic steatohepatitis. Drug Discov Today Dis Mech 2006; 3:479-488.

Adams L, Angulo P, Lindor K. Nonalcoholic fatty liver disease. Can Med Ass J 2005; 172:899-905.

Aller R, de Luis D, Fernandez L, Calle F, Velayos B, Olcoz J, Izaola O, Sagrado M, Conde R, Gonzalez J. Influence of insulin resistance and adipokines in the grade of steatosis of nonalcoholic fatty liver disease. Dig Dis Sci 2008; 53:1088-1092.

Angulo P. Obesity and nonalcoholic fatty liver disease. Nutr Rev 2007; 65:S57-S63.

Anton C, Schubert U, Bacik I, Princiotta M, Wearsch P, Gibbs J, Day P, Realini C, Rechsteiner M, Bennink J, Yewdell J. Intracellular localization of proteasomal degradation of a viral antigen. J Cell Biol 1999; 146:113-124.

Armstrong J, Blanchard G. Hepatic lipidosis in cats. Vet Clin North Am Small Anim Pract 2009; 39:599-616.

Balaban Y, Sumer H, Simsek H, Us D, Tatar G. Metabolic syndrome, non-alcoholic steatohepatitis (NASH), and hepatocyte growth factor (HGF). Ann of Hepatol 2006; 5:109-114.

Bardag-Gorce F, French B, Lue Y, Nguyen V, Wan Y, French S. Mallory bodies formed in proteasome-depleted hepatocytes: an immunohistochemical study. Exp Mol Path 2001; 70:7-18.

Bardag-Gorce F, Leeuwen F, Nguyen V, French B, Li J, Riley N, McPhaul L, Lue Y, French S. The role of the ubiquitin-proteasome pathway in the formation of Mallory bodies. Exp Mol Path 2002; 73:75-83.

Bence N, French B, Lue Y, Nguyen V, French S. Impairment of the ubiquitin-proteasome system by protein aggregation. Science 2001; 292:1552-1555.

Benoit-Biancamano M-O, Morin M, Langlois I. Histopathologic lesions of diabetes mellitus in a domestic ferret. Can Vet J 2005;46:895-897.

Bertolotti A, Zhang Y, Hendershot L, Harding H, Ron D. Dynamic interaction of BiP and ER stress transducers in the unfolded protein response. Nat Cell Biol 2000; 2:326-332.

Bjornvad C, Elnif J, Sangild P. Short-term fasting induces intrahepatic lipid accumulation and decreases intestinal mass without reduced brush-border enzyme activity in mink (*Mustela vison*) small intestine. J Comp Physiol 2004; 174B:625-632.

Bonificino J, Weissman A. Ubiquitin and the control of protein fate in the secretory and endocytic pathways. Annu Rev Cell Dev Biol 1998; 14:19-57.

Brunt E, Janney C, Di Bisceglie A, Neuschwander-Tetri B, Bacon B. Non-alcoholic steatohepatitis: A proposal for grading and staging the histological lesions. Am J Gastroenterology 1999; 94:2467-2474.

Brunt E. Pathology of nonalcoholic steatohepatitis. Hepatol Res 2005;33:68-71.

Burt A, Mutton A, Day C. Diagnosis and interpretation of steatosis and steatohepatitis. Semin Diagn Pathol 1998;15:246-258.

Burt A. Steatosis and steatohepatitis. Curr Diagn Pathol 2001; 7:141-147.

Carpenter JW, Novilla MN. Diabetes mellitus in a black-footed ferret. J Am Vet Med Assoc 1977;171:890-893.

Cederbaum S, Yu H, Grody W, Kern R, Yoo P, Iyer R. Arginases I and II: do their functions overlap? Mol Genet Metab 2004; 81:S38-S44.

Chamulitrat W, Huber A, Ridel H, Stemmel W. Nox1 makes differentiation resistance in immortalized human keratinocytes generating cells that express simple epithelial keratins. J Invest Dermatol 2007; 127:2171-2183.

Clark J, Brancati F, Diehl A. Nonalcoholic fatty liver disease. Gastroenterol 2002;122:1649-1657.

Clausen T, Olesen C, Hansen O, Wamberg S. Nursing sickness in lactating mink (*Mustela vison*). I. Epidemiological and pathological observations. Can J Vet Res 1992; 56:89-94.

Clausen TN, Sandbøl P. Correlation between liver fat and dry matter in mink (*Mustela vison*). Poster Presentation VIII International Scientific Congress in Fur Animal Production, Den Bosch, The Netherlands, September 15-18. Scientifur 2004;28:168-169.

Coux O, Tanaka K, Goldberg A. Structure and functions of the 20S and 26S proteasomes. Annu Rev Biochem 1996; 65:801-847.

Cornelius LM, Jacobs G. 1989. Feline hepatic lipidosis. In Kirk R, ed. Current Veterinary Therapy, Vol. 10. W. B. Saunders. Philadelphia.

Cuervo A. Autophagy: in sickness and health. Trends Cell Biol 2004; 14:70-77.

Cullen J, van den Ingh T, Van Winkle T, Charles J, Desmet V. 2006. Morphological classifications of parenchymal disorders of the canine and feline liver: 1 Normal histology, reversible hepatocytic injury and hepatic amyloidosis. In: Rothuizen J, Bunch

SE, Charles JA, Cullen JM, Edesmet VJ, Szatmari V, Twedt DC, van den Ingh TSGAM, Van Winkle T, Washabau RJ (Eds). WSAVA Standards for Clinical and Histological Diagnosis of Canine and Feline Liver Disease. Elsevier Philadelphia.

Damgaard B, Clausen T, Henriksen P. Effect of protein and fat content in feed on plasma alanine aminotransferase and hepatic fatty infiltration in mink. J Vet Med A 1994; 41:620-629.

Damgaard B, Clausen T, Børsting C. Effects of dietary supplement of essential amino acids on mortality rate, liver traits and blood parameters in mink (*Mustela vison*) fed low protein diets. Acta Agric Scand, Sect A, Animal Sci 1998; 48:175-183.

Day C. Pathogenesis of steatohepatitis. Best Prac Res Clin Gastroenterol 2002;16:663-678.

Day C, James O. Steatohepatitis: a tale of two "hits"? Gastroenterol 1998;114:842-845.

Day C. From fat to inflammation. Gastroenterol 2006; 130:207-210.

Denk H, Eekerstorfer R. Colchicine-induced Mallory body formation in the mouse. Lab Invest 1977; 36:563-565.

Denk H, Stumptner C, Zatloukal K. Mallory bodies revisited. J Hepatol 2000; 32:689-702.

Di Cianni G, Miccoli R, Volpe L, Lencioni C, Del Prato S. Intermediate metabolism in normal pregnancy and in gestational diabetes. Diabetes Metab Res 2003;19:259-270.

Dick M. Fatty liver syndrome in mink – causes and metabolic consequences. 2010. M.Sc. thesis. Dalhousie University, Halifax, Canada.

Dimiski D, Taboada J. Feline idiopathic hepatic lipidosis. Vet Clin North Am Small Anim Pract 1995;25:357-373.

El-Badry A, Grad R, Clavien P. Omega 3 – Omega 6: What is right for the liver? J Hepatol 2007;47:718-725.

Ellgaard L, Molinari M, Helenius A. Setting the standards: quality control in the secretory pathway. Science 1999; 286:1882-1888.

Folch J, Lees M, Sloane Stanley G. A simple method for the isolation and purification of total lipides from animal tissues. J Biol Chem 1957; 226:497-509.

Griffin B. Feline hepatic lipidosis: pathophysiology, clinical signs, and diagnosis. Compendium 2000; 22:847-858.

Gründemann D, Schömig E. Protection of DNA during preparative agarose gel electrophoresis against damage induced by ultraviolet light. BioTechniques 1996; 21:898-903.

Hanada S, Haralda M, Kumemura H, Omary M, Koga H, Kawagucki T, Taniguchi E, Yoshida T, Hisamoto T, Yanagimoto C, Maeyama M, Ueno T, Sata M. Oxidative stress induces the endoplasmic reticulum stress and facilitates inclusion formation in cultured cells. J Hepatol 2007; 47:93-102.

Hand M, Thatcher C, Remillard R, Roudebush P (Eds). 2000. Hepatobiliary disease. Pp.812- 835 in Small Animal Clinical Nutrition. Walsworth Publishing Company. Missouri.

Harada M, Kumemura H, Omary M, Kawaguchi T, Maeyama N, Hanada S, Taniguchi E, Koga H, Suganuma T, Ueno T, Sata M. Proteasome inhibition induces inclusion bodies associated with intermediate filaments and fragmentation of the golgi apparatus. Exp Cell Res 2003; 288:60-69.

Harada M, Strnad P, Toivola D, Omary M. Autophagy modulates keratin-containing inclusion formation and apoptosis in cell culture in a context-dependant fashion. Exp Cell Res 2008; 314:1753-1764.

Harding H, Zhang Y, Bertolotti A, Zeng H, Ron D. Perk is essential for translational regulation and cell survival during the unfolded protein response. Mol Cell 2000; 5:897-904.

Heid C, Stevens J, Livak K, Williams P. Real time quantitative PCR. Genome Res 1996; 6:986-994.

Hong M., Luo S., Baumeister P., Huang J., Gogia R., Li M., Lee A. Underglycosylation of ATF6 as a novel sensing mechanism for activation of the unfolded protein response. J Biol Chem 2004; 279:11354-11363.

Hübscher S. Histological assessment of the liver. Medicine 2006; 35:17-21.

Hunter B, Barker IK. Digestive System of Mink. 1996. In: Hunter B, Lemieux N (Eds). Mink … biology, health and disease. University of Guelph Graphic and Print Services, Guelph

Hunter D, Schneider R. Disease of the Lactation Period. 1996. In: Hunter B, Lemieux N (Eds). Mink … biology, health and disease. University of Guelph Graphic and Print Services, Guelph

Hynes A, Rouvinen-Watt K. Monitoring blood glucose levels in female mink during the reproductive cycle: 1. Prevention of hyperglycemia during the nursing period. Can J Vet Res 2007a; 71: 241-248.

Hynes A, Rouvinen-Watt K. Monitoring blood glucose levels in female mink during the reproductive cycle: 2. Effects of short-term fish oil, chromium picolinate, and acetylsalicylic acid supplementation during late lactation. Can J Vet Res 2007b; 71:249-255.

Iredale J. Models of liver fibrosis: exploring the dynamic nature of inflammation and repair in a solid organ. J Clin Invest 2007;117:539-548.

Johnston J, Ward C, Kopito R. Aggresomes: a cellular response to misfolded proteins. J Cell Biol 1998; 143:1883-1889.

Juokslahti T, Lindberg P, Pekkanen T, Sjogard B. Choline chloride in the treatment of fatty liver in mink. Scientifur 1978; 2:35-38.

Käkelä R, Pölönen I, Miettinen M, Asikainen K. Effects of different fat supplements on growth and hepatic lipids and fatty acids in male mink. Acta Agric Scand Sect A, Animal Sci 2001;51:217-223.

Kannan K, Newsted J, Halbrook RS, Giesy JP. Perfluorooctanesulfonate and related fluorinated hydrocarbons in mink and river otters from the United States. Environ Sci Technol 2002;36:2566-2571.

Kmiec Z. Cooperation of liver cells in health and disease. Adv Anat Embryol Cell Biol 2001; 161:1-151.

Kisselev A, Karganovich D, Goldberg A. Binding of hydrophobic peptides to several non-catalytic sites promotes peptide hydrolysis by all active sites of the 20S proteasomes. Evidence for peptide-induced channel opening in the alpha rings. J Biol Chem2002; 277: 22260-22270.

Kleiner D, Brunt E, Van Natta M, Behling C, Contos M, Cummings O, Ferrell L, Liu Y-C, Torbenson M, Unalp-Arida A, Yeh M, McCullough A, Sanyal A. Design and validation of a histological scoring system for nonalcoholic fatty liver disease. Hepatol 2005; 41:1313-1321.

Kopito R. Aggresomes, inclusion bodies and protein aggregation. Trends Cell Biol 2000; 10:524-530.

Korhonen H, Niemelä P. Effect of feeding level during autumn and winter on breeding weight and result in single and pair-housed minks. Agric Food Sci Finl 1997; 6:305-312.

Kostova Z, Wolf D. For whom the bell tolls: protein quality control of the endoplasmic reticulum and the ubiquitin-proteasome connection. EMBO J 2003; 22:2309-2317.

Kurz T, Terman A, Gustafsson B, Brunk U. Lysosomes and oxidative stress in aging and apoptosis. Biochimica et Biophysica Acta 2008; 1780:1291-1303.

Leclercq I., Morais A., Schroyen B., Van Hul1 N, Geerts A. Insulin resistance in hepatocytes and sinusoidal liver cells: Mechanisms and consequences. J Hepatol 2007; 47:142-156.

Lee A. The glucose-regulated proteins: stress induction and clinical applications. Trends Biochem Sci 2001; 26:504-510.

Lee A. The ER chaperone and signaling regulator GRP78/BiP as a monitor of endoplasmic reticulum stress. Methods 2005; 35:373-381.

Li Q, Domig K, Ettle T, Windisch W, Mair C, Schedle K. Evaluation of potential reference genes for relative quantification by RT-qPCR in different porcine tissues derived from feeding studies. Int J Mol Sci 2011; 12: 1727-1734.

Luna L. 1968. Manual of histologic staining methods of the Armed Forces Institute of Pathology. (3rd ed.). Blakison Division, McGraw-Hill Book Co., New York.

Malínská H, Oliyarnyk O, Hubová M, Zídek V, Landa V, Sîmáková M, Mlejnek P, Kazdová L, Kurtz T, Pravenec M. Increased liver oxidative stress and altered PUFA metabolism precede development of non-alcoholic steatohepatitis in SREBP-1a transgenic spontaneously hypertensive rats with genetic predisposition to hepatic steatosis. Mol Cell Biochem 2010; 335:119-125.

Mantena S, King A, Andringa K, Eccleston, Bailey H. Mitochondrial dysfunction and oxidative stress in the pathogenesis of alcohol and obesity-induced fatty liver diseases. Free Radic Biol Med 2008; 44: 1259-1272.

Mantena S, Vaughn D, Andringa K, Eccleston H, King A, Abrams G, Doeller J, Kraus D, Darley-Usmar V, Bailey S. High fat diet induces dysregulation of hepatic oxygen gradietns and mitochondrial function in vivo. Biochemical Journal. 2009;417:183-193.

Marceau P, Biron S, Hould FS, Marceau S, Simard S, Thung SN, Kral JG. Liver pathology and the metabolic syndrome X in severe obesity. J Clin Endocrinol Metab 1999;84:1513-1517.

Merat S, Khadem-Sameni F, Nouraie M, Derakhshan M, Mohammad Tavangar S, Mossaffa S, Malekzadeh R, Sotoudeh M. A modification of the Brunt system for scoring liver histology of patients with non-alcoholic fatty liver disease. Arch Iran Med 2010; 13: 38-44.

McCuskey RS, Ito Y, Robertson GR, McCuskey MK, Perry M, Farrel GC. Hepatic microvascular dysfunction during evolution of dietary steatohepatitis in mice. Hepatol 2004;40:386-393.

Michalik A, Van Broeckhoven C. Pathogenesis of polyglutamine disorders: aggregation revisited. Hum Mol Genet 2003; 12:R173-R186.

Mitchell J, Rouvinen-Watt K. Body condition, liver fat and liver glycogen of wild American mink (*Neovison vison*) in Nova Scotia, Canada. IX International Scientific Congress in Fur Animal Production. International Fur Animal Scientific Association. Halifax, NS, Canada. August 19-23, 2008. Scientifur 2008;32:217-218.

Mori K. Tripartite management of unfolded proteins in the endoplasmic reticulum. Cell 2000; 101:451-454.

Mustonen A-M, Puukka M, Nieminen P. Adaptations to fasting in the American mink (*Mustela vison*): nitrogen metabolism. J Comp Physiol B 2005a; 175:357-363.

Mustonen A-M, Pyykönen T, Paakkonen T, Ryökkynen A, Asikainen J, Aho J, Mononen J, Nieminen P. Adaptations to fasting in the American mink (*Mustela vison*): carbohydrate and lipid metabolism. Comp Biochem Physiol A 2005b; 140:195-202.

Mustonen A-M, Puukka M, Saarela S, Paakkonen T, Aho J, Nieminen P. Adatations to fasting in a terrestrial mustelid, the sable (*Martes zibellina*). Comp Biochem Physiol A 2006; 144:444-450.

Mustonen A-M, Puukka M, Rouvinen-Watt K, Aho J, Asikainen J, Nieminen P. Response to fasting in an unnaturally obese carnivore, the captive European polecat Mustela putorius. Exp Biol Med 2009; 234:1287–1295.

Nieminen P, Rouvinen-Watt K, Collins D, Grant J, Mustonen A-M. Fatty acid profiles and relative mobilization during fasting in adipose tissue depots of the American marten (*Martes americana*). Lipids 2006; 41:231-240.

Nieminen P, Mustonen A-M, Kärjä V, Asikainen J, Rouvinen-Watt K. Fatty acid composition and development of hepatic lipidosis during food deprivation – mustelids as a potential animal model for liver steatosis. Exp Biol Med 2009; 234:278-286.

Nieminen P, Rouvinen-Watt K, Kapiainen S, Harris L, Mustonen A-M. Molecular evolution of adiponectin in Carnivora and its mRNA expression in relation to hepatic lipidosis. Gen Comp Endocrinol 2010; 168:307-311.

Omary M, Ku N, Toviola D. Keratins: guardians of the liver. Hepatol 2002; 35:251-257.

Özcan U, Cao Q, Yilmaz E, Lee A-H, Iwakoshi N, Özdelen E, Tuncman G, Görgün C, Glimcher L, Hotamisligil G. Endoplasmic reticulum stress links obesity, insulin action, and type 2 diabetes. Science 2004; 306:457-461.

Pal C, Nieminen P, Mustonen A-M, Rouvinen-Watt K. 2008. Effects of fasting and re-feeding on the development of hepatic lipidosis in the American mink (*Neovison vison*). IX International Scientific Congress in Fur Animal Production. International Fur Animal Scientific Association. Halifax, NS, Canada. August 19-23. Scientifur 32:219-220. IFTF

Powell E, Cooksley W, Hanson R, Searle J, Halliday J, Powell W. The natural history of nonalcoholic steatohepatitis: a follow-up study of forty-two patients for up to 21 years. Hepatol 1990;11:74-80.

Pulsinelli W, Waldman S, Rawlinson D, Plum F. Moderate hyperglycemia augments ischemic brain damage:A neuropathologic study in the rat. Neurol 1982; 32: 1239-1246.

Ravikumar B, Duden R, Rubinsztein D. Aggregate-prone proteins with polyglutamine and polyalanine expansions are degraded by autophagy. Hum Mol Genet 2002; 11:1107-1117.

Reddy R, Dubeau L, Kleiner H, Parr T, Nichols P, Ko B, Dong D, Ko H, Mao C, KiGiovanni J, Lee A. Cancer inducible transgene expression by the GRP94 promoter: spontaneous activation in tumors of various origins and cancer-associated macrophages. Cancer Res 2002; 62:7207-7212.

Reeves H, Friedman S. Activation of hepatic stellate cells - a key issue in liver fibrosis. Front BioSci 2002; 7:808-826.

Roberts R, Ganey P, Ju C, Kamendulis L, Ruysn I, Klaunig J. Role of the Kupffer cell in mediated hepatic toxicity and carcinogenesis. Toxicol Sci 2007; 96:2-15.

Rock K, Gramm C, Rothstein L, Clark L, Stein R, Dick L, Hwang D, Goldberg A. Inhibitors of proteasome block the degradation of most cell proteins and the generation of peptides on MHC class I molecules. Cell 1994; 78:761-771.

Ross M, Pawlina W. 2006. Digestive system III: Liver, Gallbladder, and Pancreas. P576-602. in Histology a text and atlas with correlated cell and molecular biology. Lippincott Williams & Wilkins. Baltimore.

Rouvinen K, Kiiskinen T. Influence of dietary fat source on the body fat composition of mink (*Mustela vison*) and the blue fox (*Alopex lagopus*). Acta Agric Scand 1989; 39:279-288.

Rouvinen-Watt K. Nursing sickness in the mink (*Mustela vison)* – a metabolic mystery or a familiar foe? Review Article. Can J Vet Res 2003; 67:161-168.

Rouvinen-Watt K, Murphy J, Chan C. Effect of feeding intensity on body condition and glycemic control in mink *Mustela vison*. Proceedings of the VIII International Scientific

Congress in Fur Animal Production, De Ruwenberg, 's-Hertogenbosch, The Netherlands, 15-18 September 2004. Scientifur 2004;28:129-135.

Rouvinen-Watt K, Mustonen A-M, Conway R, Pal C, Harris, L, Saarela S, Strandberg U, Nieminen P. Rapid development of fasting-induced hepatic lipidosis in the American mink (*Neovison vison*): effects of food deprivation and re-alimentation on body fat depots, tissue fatty acid profiles, hematology and endocrinology. Lipids 2010; 45:111-128.

Scheuer P, Lefkowitch J. 2000. Steatosis and Steatohepatitis. Pp21-34, 105-123 in Liver Biopsy Interpretation. W.B. Saunders Company. Philadelphia.

Schneider R, Hunter D, Waltner-Toews D. Nursing disease in mink: ranch level epidemiology. Pre Vet Med 1992; 14:181-194.

Shoelson S, Lee J, Goldfine A. Inflammation and insulin resistance. J Clin Invest 2006; 116:1793-1801.

Sitia R, Braakman I. Quality control in the endoplasmic reticulum protein factory. Nature 2003; 426:891-894.

Sjastaad VO, Hove K, Sand O. 2003. Physiology of Domestic Animals. Scandinavian Veterinary Press, Oslo.

Smith DG, Schenk MP. Dissection Guide and Atlas to the Mink. 2000. Morton publishing Company, Colorado.

Sriburi R, Jackowski S, Mori K, Brewer J. XBP1: a link between the unfolded protein response, lipid biosynthesis, and biogenesis of the endoplasmic reticulum. J Cell Biol 2004; 167:35–41.

Svobodova K, Bilek K, Knoll A. Verification of reference genes for relative quantification of gene expression by real-time reverse transcription PCR in the pig. J Appl Genet 2008; 49: 263-265.

Tannapfel A, Denk H, Dienes H-P, Langner C, Schirmacher P, Trauner M, Flott-Rahmel B. Histopathological diagnosis of non-alcoholic and alcoholic fatty liver disease. Virchows Arch 2011; 458:511-523.

Taylor J, Hardy J, Fischbeck K. Toxic proteins in neurodegenerative disease. Science 2002; 296:1991-1995.

Tauson A. Pre-mating body weight changes and reproductive performance in female mink. Acta Agric Scand 1984; 34:177-187.

Thom MD, Harrington LA, Mcdonald DW. Why are American mink sexually dimorphic? A role for niche separation. Oikos 2004; 105:525-535.

Tilg H. Adipocytokines in nonalcoholic fatty liver disease: key players regulating steatosis, inflammation and fibrosis. Curr Pharm Des 2010; 16:1893-1895.

Toshimitsu K, Matsuura B, Ohkubo I, Niiya T, Furukawa S, Hiasa Y, Kawamura M, Ebihara K, Onji M. Dietary habits and nutrient intake in non-alcoholic steatohepatitis. Nutr 2007;23:46-52.

Travers K, Patil C, Wodicka L, Lockhard D, Weissman J, Walter P. Functional and genomic analysis reveal an essential coordination between the unfolded protein response and ER associated degradation. Cell 2000; 101:249-258.

Videla L, Rodrigo R, Araya J, Poniachik J. Oxidative stress and depletion of hepatic long-chain polyunsaturated fatty acids may contribute to non alcoholic fatty liver disease. Free Radic Biol Med 2004; 37:1499-1506.

Wamberg S, Clausen TN, Olesen CR, Hansen O. Nursing sickness in lactating mink (*Mustela vison*) II. Pathophysiology and changes in body fluid composition. Can J Vet Res 1992;56:95-101.

Wasserback York L, Puthalapattu S, Wu G. Nonalcoholic fatty liver disease and low-carbohydrate diets. Annu Rev Nutr 2009;29:365-379.

Webb J, Ravikumar B, Atkins J, Skepper J, Rubinsztein D. α-Synuclein is degraded by both autophagy and the proteasome. J Biol Chem 2003; 278:25009-25013.

Westphal S. Obesity, abdominal obesity, and insulin resistance. Clin Cornerstone 2008; 9:23-31.

Wigley W, Fabunni R, Lee M, Marino C, Muallem S, DeMartino G, Thomas P. Dynamic association of proteasomal machinery with the centrosome. J Cell Biol 1999; 145:481-490.

Wong M, Medrano J. Real-time PCR for mRNA manipulation. BioTechniques 2005; 39: 75-85.

Yuan Q, Nagao Y, Gaal K, Hu B, French S. Mechanism of Mallory body formation induced by okadaic acid in drug-primed mice. Exp Mol Pathol 1998; 65:87-103.

Zatloukal K, Spurej G, Rainer I, Lackinger E, Denk H. Fate of Mallory body-containing hepatocytes: disappearance of Mallory bodies and restoration of the hepatocyte intermediate filament cytoskeleton after drug withdrawl in the griseofulvin-treated mouse. Hepatol 1990; 11:652-661.

Zatloukal K, Stumptner A, Fuchsbichler E, Janig E, Denk H. Intermediate filament protein inclusions. Methods Cell Biol 2004a; 78:205-228.

Zatloukal K, Stumptner C, Fuchsbichler A, Fickert P, Lackner C, Trauner M. The keratin cytoskeleton in liver diseases. J Pathol 2004b; 204:367-376.

Zatloukal K, French S, Stumptner C, Strnad P, Harada M, Toivola D, Cadrin M, Omary M. From Mallory to Mallory-Denk bodies: What, how and why? Exp Cell Res 2007; 313:2033-2049.